

8-1983

# Analytical Pyrolysis of Eastern Shales

Kenneth Naples

*Western Kentucky University*

Follow this and additional works at: <https://digitalcommons.wku.edu/theses>



Part of the [Chemistry Commons](#)

---

## Recommended Citation

Naples, Kenneth, "Analytical Pyrolysis of Eastern Shales" (1983). *Masters Theses & Specialist Projects*. Paper 2695.  
<https://digitalcommons.wku.edu/theses/2695>

This Thesis is brought to you for free and open access by TopSCHOLAR®. It has been accepted for inclusion in Masters Theses & Specialist Projects by an authorized administrator of TopSCHOLAR®. For more information, please contact [topscholar@wku.edu](mailto:topscholar@wku.edu).

Naples,

Kenneth V.

1983

ANALYTICAL PYROLYSIS OF EASTERN SHALES

A Thesis

Presented to

the Faculty of the Department of Chemistry

Western Kentucky University

Bowling Green, Kentucky

In Partial Fulfillment

of the Requirements for the Degree

Master of Science

by

Kenneth V. Naples

August 1983

**AUTHORIZATION FOR USE OF THESIS**

Permission is hereby

granted to the Western Kentucky University Library to make, or allow to be made photocopies, microfilm or other copies of this thesis for appropriate research or scholarly purposes.

reserved to the author for the making of any copies of this thesis except for brief sections for research or scholarly purposes.

Signed Kenneth V. Peoples

Date July 15/83

Please place an "X" in the appropriate box.

This form will be filed with the original of the thesis and will control future use of the thesis.

ANALYTICAL PYROLYSIS OF EASTERN SHALES

Recommended July 7, 1983  
(Date)

John W. Season  
Director of Thesis

John T. Riley

J. Boucher

Approved 8-5-83  
(Date)

Almer Gray  
Dean of the Graduate College

## ACKNOWLEDGEMENTS

I would like to express my deepest appreciation to the following people who all took part in the formation of this thesis:

Dr. John Reasoner whose patience, vigilance, guidance and tutelage over the research of this thesis was a personal inspiration to me.

Dr. Marshall J. Margolis of IMMR, Lexington, Kentucky, for his help with the project.

Ms. Mary B. Harris of IMMR, Lexington, Kentucky, for the thermogravimetric analysis on spent shales.

Mr. Gerald Thomas of IMMR, Lexington, Kentucky, for elemental analysis on spent shales.

The Institute for Mining and Minerals Research for financial support in the form of UKRF Contract No. 54502-91-56.

To the following people, I would like to offer my personal and eternal gratitude:

Dr. Robert Farina, who convinced me to come to Western Kentucky University.

Sister Jean, through her own example, showed me how to make the transition.

Ms. Jean Almond for her excellent service in helping me to procure the background literature for this thesis.

The entire Department of Chemistry of Western Kentucky University for their instruction, par excellence, as well as their accomodating my endless questions.

Ray Hsu, of the Department of Mathematics of Western Kentucky University, whose knowledge of computer programming helped in the compilation of my statistical data of this thesis.

To all my graduate colleagues: Jana, John, Joe, Liz, Vicki, Bijhan, Ann, Eduardo, Eric, Pablo, Alvaro, Randy, Carol, Kevin, Terry, Steve, Bob and Tom whose warm fellowship made my year of study at Western Kentucky University a gratifying experience.

Ms. Judy Campbell for the final typing of this thesis.

## DEDICATION

This is dedicated to my loving wife, Joan, and my children: Susan, Nancy, Anne and Kenny, Jr., whose infinite support made the writing of this thesis possible.

## TABLE OF CONTENTS

Chapter	Page
I. INTRODUCTION . . . . .	1
II. HISTORICAL . . . . .	3
III. EXPERIMENTAL . . . . .	30
Oil Shales . . . . .	30
Instrumentation . . . . .	31
Procedure . . . . .	31
Pyroprobe Calibration . . . . .	35
IV. RESULTS . . . . .	40
V. DISCUSSION . . . . .	54
VI. SUMMARY . . . . .	71
VIII. BIBLIOGRAPHY . . . . .	72

## LIST OF FIGURES

Figure	Page
1. Model of How Western Shale was Formed . . . . .	10
2. A Modified Fischer Assay Apparatus . . . . .	19
3. Free Radicals Combining with Combined Hydrogen to Form Oils . . . . .	18
4. Disproportionation of Larger Molecules . . . . .	20
5. Free Radicals Combining to Form Char or Coke .	21
6. Chemical Data Systems 820 Reaction System . .	24
7. Pyrogram of La Luna Shale P <sub>1</sub> . . . . .	25
8. Pyrogram of Posidonien Shale . . . . .	26
9. Pyrogram of La Luna Shale P <sub>2</sub> . . . . .	28
10. Pyrogram of Posidonien Shale P <sub>2</sub> . . . . .	29
11. Typical Pyrogram Showing High Volatile and Low Volatile Fractions . . . . .	34
12. The Levy-Walker Molecular Thermometer Calibration Curve for Kraton 1107 Polymer . . . . .	38
13. Reaction between Styrene and Phenoxy Radicals to Form Methane and Propene; Ethane and Ethene .	57
14. Mechanism Showing the Desproportionation of Butane to Form Methane and Propene; Ethane and Ethene . . . . .	58
15. Reaction between a Styrene Radical and Phenoxy Radical in Forming Beta Phenoxy Ethyl Benzene . . . . .	59
16. Percent Carbon Removal vs Heating Rate . . . . .	65

## LIST OF TABLES

Table		Page
1.	Results of Tests on Devonian Shales under Oil-Producing Conditions . . . . .	16
2.	Results of Tests on Devonian Shales under Gas-Producing Conditions . . . . .	17
3.	Elemental and Thermal Gravimetric Analysis . .	30
4.	Results of Experiments for Levy-Walker Calibration Curve . . . . .	37
5.	Experimental Results using Ceiling Temperature of 550°C . . . . .	40
6.	Experimental Results using Ceiling Temperature of 650°C . . . . .	41
7.	Experimental Results using Ceiling Temperature of 750°C . . . . .	41
2	Tables 8-17: Experimental Results of Effect of Heating Rates of:	
8.	Cleveland at 10°C/min. (Approx. Fischer Assay)	43
9.	Sunbury at 10°C/min. (Approx. Fischer Assay)	43
10.	Cleveland at 120°C/min. . . . .	44
11.	Cleveland at 300°C/min. . . . .	44
12.	Cleveland at 100°C/sec. . . . .	45
13.	Cleveland at 600°C/sec. . . . .	45
14.	Sunbury at 120°C/min. . . . .	46
15.	Sunbury at 300°C/min. . . . .	46
16.	Sunbury at 100°C/sec. . . . .	47
17.	Sunbury at 600°C/sec. . . . .	47
18.	Carbon-Hydrogen-Nitrogen and Thermo-Gravimetric Analtsis on Spent Cleveland Shale . . . . .	49

Table	Page
19. Elemental and Thermo-Gravimetric Analysis on Spent Sunbury Shale . . . . .	50
Tables 20-23: Experimental Results of Effects of Mesh Size on Cleveland Shale	
20. -30 Mesh . . . . .	51
21. 30/60 Mesh . . . . .	51
22. 60/100 Mesh . . . . .	52
23. -100 Mesh . . . . .	52
24. Elemental and Thermo-Gravimetric Analysis	53
25. Summary of Product Yield and Distribution as a Function of Ceiling Temperature on Sunbury Shale . . . . .	56
26. Summary of Experimental Results of Effects of Heating Rates on Cleveland Shale . . . . .	61
27. Summary of Experimental Results of Effects of Heating Rates on Sunbury Shale . . . . .	61
28. Analysis of the Spent Cleveland Shale as a Function of the Heating Rate . . . . .	62
29. Analysis of the Spent Sunbury Shale as a Function of the Heating Rate . . . . .	63
30. Experimental Results of Product Yield and Distribution as a Function of the Mesh Size on Cleveland Shale . . . . .	67

## ANALYTICAL PYROLYSIS OF EASTERN OIL SHALES

Kenneth V. Naples

August 1983

75 pages

Directed by: Dr. John W. Reasoner, John T. Riley and

Laurence J. Boucher

Department of Chemistry

Western Kentucky University

The effects of pyrolysis interval, ceiling temperature, heating rate and mesh size on both the pyrolysis yield and relative product distribution for two eastern oil shales (Sunbury and Cleveland) were studied. An extension of the technique of analytical pyrolysis (pyrolysis-gas chromatography) was used. This extension employed a Chemical Data System (C.D.S.) Model 382 Extended Pyroprobe and a C.D.S. Model 310 Concentrator which enabled the pyrolysis products to be collected into a trap system. After completion of a predetermined heating interval, the trap was pulse heated to 250°C and the high and low volatile components were back-flushed into the injection port of a Varian Model 3700 Gas Chromatograph and separated into the low and high molecular weight fractions respectively. Measurements of relative peak areas of the pyrogram gave the yield of the respective fractions.

Samples were repeatedly pulsed to obtain intervals of up to 120 seconds at ceiling temperatures of 750°C for both shales and a ceiling temperature of 550°C for the Cleveland shale.

Ceiling temperatures of 550°C, 650°C, and 750°C, with an interval of 20 seconds were investigated for the Sunbury Shale only to test the concentrator system.

Ramps of 10°C/min, 120°C/min, 300°C/min, 100°C/sec, and a nonlinear ramp of 600°C/sec were employed for both the Sunbury and Cleveland shales at a ceiling temperature of 500°C for an interval of 60 minutes. The 10°C/min ramp is a close approximation of the Fischer Assay conditions.

Mesh sizes of -30, 30/60, 60/100, -100 were studied for the Cleveland shale only. Data was collected for each mesh size at a ceiling temperature of 650°C and an interval of 20 seconds.

Carbon-hydrogen-nitrogen and thermogravimetric analyses were also performed on the spent shale. The results of the above investigation may be summarized as follows:

1. At lower ceiling temperatures, the heating interval has to be increased in order to maintain optimum yields of product.

2. As the ceiling temperature increases, the overall product yield increases.

3. There is a shift in product distribution towards the high volatile fraction (lower molecular weights) with higher rates of heating and higher ceiling temperature.

4. The optimum heating rate for the eastern oil shales studied appears to be between 120° and 300°C per minute.

5. These experiments suggest that pyrolysis of smaller mesh samples results in a slight yield enhancement. It is also probable that the finer mesh shales are also more susceptible to oxidative aging.

## INTRODUCTION

Today and in the future, there is an increasing need for the United States to be independent of imported oil. Shale oil is one resource that can help meet this need. Its importance is manifested by the fact that the United States contains 8 percent of the world's  $4 \times 10^{18}$  Kg of the mineral. (1)

There are two principal areas of concentrated shale in the United States. These are:

1. The Green River Formation, which encompasses  $4.5 \times 10^6$  ha of Colorado, Wyoming, and Utah, has a potential yield of  $1.3 \times 10^{12}$  m<sup>3</sup> of oil.
2. The Devonian and Mississippian deposits ranging from Western New York, Michigan to West Texas. The Devonian deposits are approximately 350 million years old while those of the Mississippian Age are about 260 million years old.

Although western shale deposits yield about 2.5 times as much oil as eastern shale, there are certain conditions that restrict the development of them. One constraint is the lack of water for processing shale and for land reclamation. Another is the lack of an established labor force in the sparsely populated western areas. This makes the development of eastern shales, where water and labor are both abundant, more practical. (2)

It is desirable, therefore, to optimize oil yields from these eastern oil shales during processing. Variables that affect overall product yield include ceiling temperature, ramp, heating interval and particle size. Very little work has been done to study the effect of these parameters on the oil yield from eastern oil shale. The purpose of this project was to investigate the effect of the above parameters on product yield and distribution for two representative eastern oil shales.

## HISTORICAL

Many authorities define oil shale as an organic rich mineral which yields a minimum of 38 litres or 10 U.S. gallons per ton of shale.

All oil shales contain "kerogen" which is a high molecular weight organic polymer, insoluble in common organic solvents and formed from algal (marine) deposits.<sup>(3)</sup> When viewed under a microscope, kerogen appears as a dark waxy, shapeless material in which small brilliant yellow, red, or green particles are dispersed. These particles are finely ground fossil remains of spores, pollen, filaments of algae, and parts of plants or animals.<sup>(4)</sup> Surrounding the kerogen are inorganic materials such as: Dolomite-Ankerite ( $\text{Mg, Fe}[\text{Ca}(\text{CO}_3)]$ ), Calcite ( $\text{CaCO}_3$ ), Quartz ( $\text{SiO}_2$ ), Iron Pyrite ( $\text{FeS}_2$ ), Illite [ $(\text{OH})_4 \text{K}_2(\text{Si}_6\text{Al}_2) \text{Al}_4 \text{O}_{20}$ ] and various silicates. The variations in compositions of the inorganic material can be used to characterize different shales. This variation will be illustrated later when eastern shale is compared to western shale.

Kerogen can be characterized by using a technique called "pyrolysis." Pyrolysis can be defined as the decomposition of organic matter by heat in the absence of air. By pyrolyzing three kinds of kerogen (Marine, Terrestrial or a mixture of both) the following has been observed:

1. Marine Kerogens yield largely aliphatic compounds in the form of short straight or branched carbon chains in the form of paraffins, olefins, ketones, etc.
2. Terrestrial Kerogens yield more aromatic and phenolic products in the form of alkyl-phenols and methoxy phenols, along with longer chain alkanes and alkenes with odd and even carbon numbers, respectively. (5)

In all the samples pyrolyzed it was shown that the kerogen also yielded large quantities of gaseous products such as  $\text{CH}_4$ ,  $\text{CO}_2$ ,  $\text{H}_2\text{S}$ , and  $\text{SO}_2$ . Also, it is interesting to note that the n-alkane and n-alkene concentration increases with increasing geological age while the Phenolic concentration of the kerogen decreases.

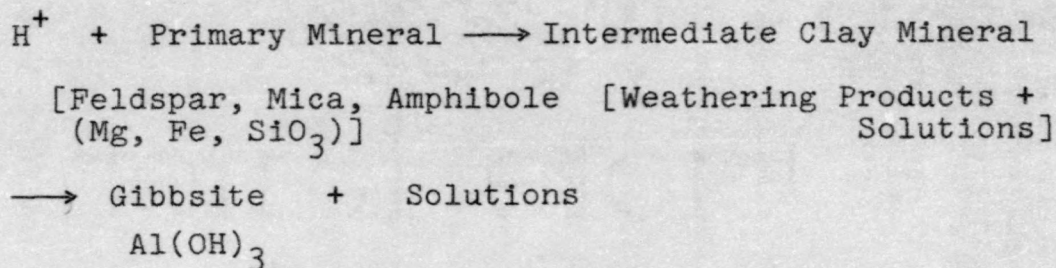
Presently, the United States annual rate of oil consumption is approximately  $9 \times 10^8 \text{ m}^3$ . The potential yield of oil shale is as follows:

$$\begin{array}{r}
 \text{Western oil yield} = 1.3 \times 10^{12} \text{ m}^3 \\
 \text{Eastern oil yield} = .5 \times 10^{12} \text{ m}^3 \\
 \hline
 \text{Total Resources} = 1.8 \times 10^{12} \text{ m}^3 \quad (6)
 \end{array}$$

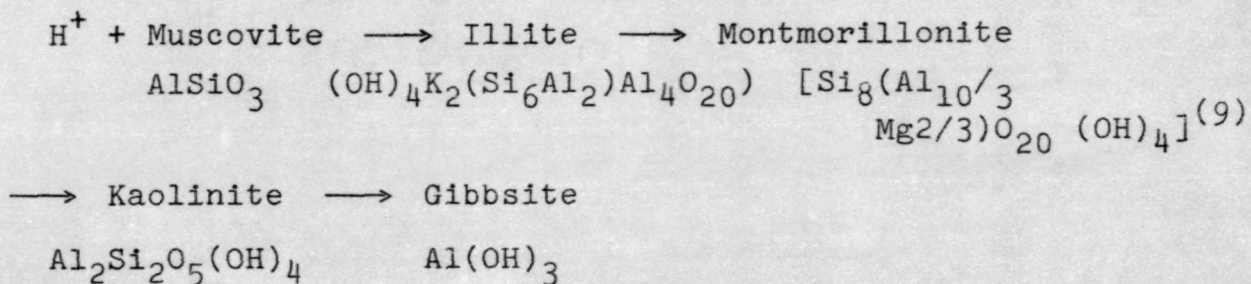
At the present consumption rate, this supply could last for approximately 2,000 years. However, if shale oil production is limited to  $64,000 \text{ m}^3/\text{day}$ , due to environmental controls, the supply would last approximately 77,000 years. The figure  $64,000 \text{ m}^3/\text{day} = 2.3 \times 10^7 \text{ m}^3/\text{yr}$ , representing approximately 2.6% of our annual need, suggests that improvements in our present technology must be made if shale oil is to have a significant impact on our present oil demands.

The formation of oil shale is caused by the accumulation of layers of mud and various organisms on the bottom of ancient lakes, ponds, and shallow seas. These waters were fairly stagnant causing the limited supply of oxygen to promote the slow decomposition of the dead organisms. Over a long geological period of time, younger sediments were deposited on top of these muds and the resulting increased pressure compacted them into hard shale. (7)

The origin of these muds may have been formed from the erosion of pre-existing muds, mudstones and shales; the weathering of silicates; abrasive action by glaciers and the pulverization and ingestion of sediment by organisms. Clay minerals can form from the weathering of primary minerals in the following general way. (8)



A Specific Example:



The deposition of muds are in the form of either flocculates or aggregates. (10) Flocculates are clay particles

caused by a chemical reaction with salt water to form fuzzy microscopic spheres or groups, whereas aggregates are groups of clay particles which are cemented together.

Flocculates and aggregates are determined by the water chemistry, particle size and shapes, fluid turbulence, suspension concentration,<sup>(11)</sup> mineralogy of particles,<sup>(12,13)</sup> gravity flow and suspension transport.<sup>(14)</sup>

Muds can accumulate in protected basins irrespective of water depth, along shore lines and protective topographical lows, on shelves from shore-lines and in deep ocean basins.

Once the muds are deposited, cohesion of the mud begins. The nature of this cohesion is principally the electrostatic attractions between the charged particles at the boundaries of the clay particles and the water molecules that are in between them. The muds resist erosion and become horizontally stratified into different sedimentary structures where vertical differences are distinguished by differences in color and hardness. Horizontal layers can be separated by weathering, a process called "parting." The stratification is divided into two thicknesses. Layers which are greater than 10 mm thick are called "beds," and layers less than 10 mm thick are called "laminae." McKee and Weir (1953) noted that the less laminated the shale, the more clay and organic content it possesses and the more bedded the shale, the more sand, silt and carbonates occur within its structure.<sup>(15)</sup>

Potter, Maynard and Pryor have organized sedimentary structures associated with both shales and interbedded shales, sandstones and carbonates into three genetic groups:

1. Sedimentary structures that are primarily formed from hydraulic processes.
2. Sedimentary structures that are formed after deposition by fluid loss, compaction and deformational processes.
3. Diagenetic structures formed by chemical processes some of which form very soon after deposition. (16)

The authors have shown the various stratification types whose variances can determine the differential settling rates of various constituents and can determine whether deposition of clay particles flocculate or aggregate. (17)

Beds and laminae show variances in the history of deposition through changes in water chemistry that affects organic productivity and controls the precipitation of minerals. For example, algal bedding in carbonates is an example of bedding produced by carbonate-trapping organisms that are sensitive to both water chemistry and light. (18)

Compactional and deformation structures are records of events and conditions in the environment between depositional events. They are formed by the following: gravitational movements, density differences, intergranular fluid movement, desiccation processes; for example, muds are prone to "soft-sediment" deformation because pore water pressure does not dissipate rapidly through low permeable muds. (19)

Diagenetic structures show the geochemical character of ancient substrates. They are useful in estimating the degree of compaction in shale and are concretionary in nature, being composed of such minerals as: Calcite, Dolomite, Hematite,

Pyrite, Gypsum and Barite.<sup>(20,21)</sup> These concretions are associated with organic compounds of animal or plant fossils.<sup>(21)</sup> Precipitation of mineral matter can either displace host rock, occupy the pore space of the host rock only, or occur in voids and open fractures. Also, mineral matter can precipitate syngenetically at the sedimentary water interface.<sup>(23)</sup> The character of the host shale will provide the best clue of determining the kind of precipitation.<sup>(24)</sup> Mechanistically, Weeks (1953) suggests that when organic tissues decay, ammonia is produced and increases the pH high enough so that calcium carbonate will precipitate from the pore fluids and will form a nodule around the organic matter prior to compaction.<sup>(25)</sup> This mechanism was verified by Berner (1968).<sup>(26)</sup>

Once the inorganic content and the nature of the rock constituent of shale has been established, one only has to look at the origin of the organic material which is entrapped in the host rock in order to understand completely the formation of oil shale.

Organisms determine the hydrocarbon content of a shale.<sup>(27)</sup> Originally, they resided in the nutrient rich muds which are the precursor of shale. Marine organisms and bacteria contribute lipid-rich organic matter, whereas terrestrial plant detritus--for example, spores, pollen, and cuticles--contribute lignin-rich organic matter. The quantity of organic matter is a function of biological productivity which is controlled by optimum conditions of light, temperature, and mineral nutrients such as phosphorus and nitrates as well as by the preservation of organic matter after the death of the organism.

These conditions occur in shaley basins where sedimentation is high and oxygenation rates are low.<sup>(28)</sup> As explained earlier, this fossilization makes up both the kerogen and the volatiles contained in shale. Van De Meent, Brown, Philip and Sinoneit (1979) have characterized the kerogens of a series of oil shales according to its organic matter and its origin.<sup>(29)</sup>

In comparing the shale from the eastern United States to those in the western United States, one has to look at the environments from which each of these two respective shales were formed. Western shale was formed from a fresh water environment whereas eastern shale was formed from a salt water environment. Thus, because of differences in their respective marine life, western shale contains more carbonates and is more porous than the closely compacted eastern shale. Western shale, particularly the green river shale, is composed of marlestons deposited from a lucustrine brackish water environment during the Eocene period of 50 million years ago. The increase in water salinity formed beds of saline minerals. As indicated in Figure 1,<sup>(30)</sup> precipitation would cause sediments to flow down the sides of the mountains into neighboring lakes where fish, fresh water invertebrates, crustaceans, snails, and clams abounded. These wet periods were followed by extreme arid conditions which caused the water of these lakes to recede to form shallow lakes (playa lakes) and large mud flats, where large cracks would form.

Playa lake model for deposition of the Green River oil shale and interbedded evaporites. Vertical scale greatly exaggerated.

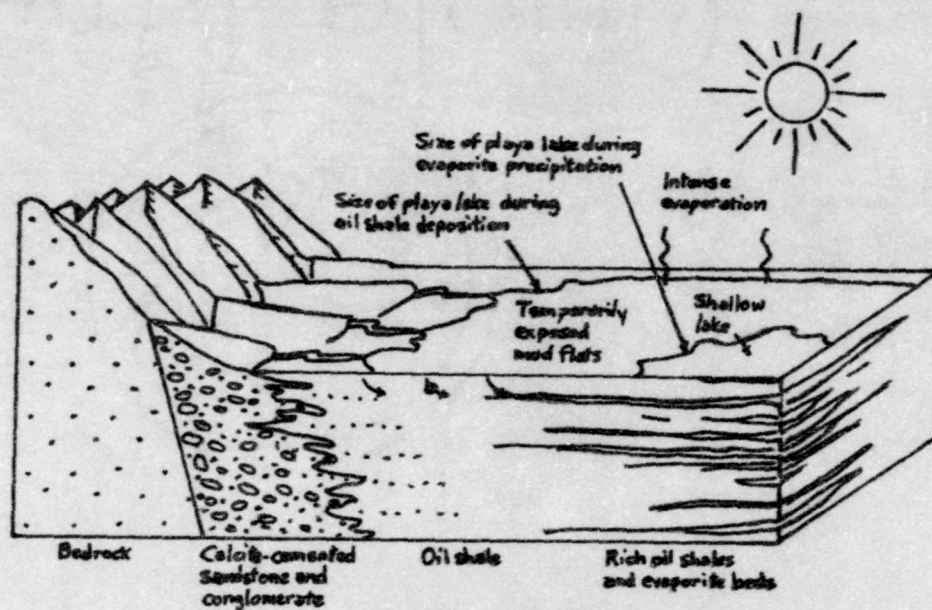


FIGURE 1. Model of How Western Shale was Formed.

Organisms would fall in the cracks and carbonates contained in brine would precipitate in the lakes as evaporite minerals. These minerals would include: Halite ( $\text{NaCl}$ ), Trona [ $\text{Na}_2 \text{CO}_3 \text{ Na H CO}_3 (\text{H}_2\text{O})$ ], Calcite ( $\text{CaCO}_3$ ), Nahcolite ( $\text{Na HCO}_3$ ), Dolomite [ $\text{Ca Mg} (\text{CO}_3)_2$ ] and Dawsonite [ $\text{Na Al}(\text{CO}_3)_3 2\text{Al}(\text{OH})_3$ ]. When the wet periods would follow the dry eras the playa lakes would expand and further sedimentation would fill in the mud cracks.

After several cyclical periods, enough sediments would be deposited to provide the necessary pressure to compact the blue-green algae, organisms and other aquatic flora and fauna into the oil shale. The organic material from the algae is the main constituent in the kerogen of the green river oil shale, and yields of 15 or more gallons of oil per ton are reported. It is estimated that  $1,800 \times 10^9$  barrels of shale oil are contained by the green river formation. (31)

Much of the eastern United States was covered by the shallow inland Chattanooga Sea about 330-360 million years ago. These stagnant waters contained very rich algae and humic growth which were probably responsible for the organic matter contained in the black shale. The humic materials originating from terrestrial plant life were deposited close to shore and the algae distribution extended throughout a three basin area. It is notable that organic matter derived from algae gives a higher Fischer assay oil yield than that of the humic organic matter. This is because the humic matter, composed mainly of cellulose and lignin, contains less hydrogen and more oxygen than its algae counterpart.

Eastern shale is the product of a continuous slow deposition of carbonaceous black mud from the down warping of the Appalachian geosyncline and the erosion of the mountainous eastern landmass. This erosion is probably responsible for the coarse sandstones and red beds found along the eastern edge of the geosyncline. These beds are diluted with river-borne sediments or clastics.

Since eastern shales are formed from muds, it is reasonable to assume that various clay minerals such as kaolinite, smectite, illite, muscovite, quartz, and pyrite are associated with the host rock.

The United States Geological Survey reported that the Devonian oil shale in the eastern United States is estimated to be  $400 \times 10^9$  barrels of oil of known resources. This figure could be extended to  $2600 \times 10^9$  barrels as development of these shales progresses. (32)

Although oil shale had been used for domestic purposes since the 14th century in Europe, the first oil shale industry did not appear until the mid 19th century. France, in 1838, began to produce lamp fuel by distilling oil shale. Later, in 1862, oil from shale was produced in Scotland. The oil shale industry continued to develop there for one hundred years, peaking at a production rate of one million litres of oil per day in 1913. Meanwhile, other countries began developing their own oil shale resources. In 1921, Estonia produced gas and oil from shale for electrical power. In 1929, Manchuria began producing oil, and while under the control of Japan during World War II, it reached a production rate

of  $575 \times 10^3$  litres per day of crude shale oil. During the 1970's China had expanded its output of shale oil to between  $6.5 \times 10^6$  and  $9.5 \times 10^6$  litres per day. (33)

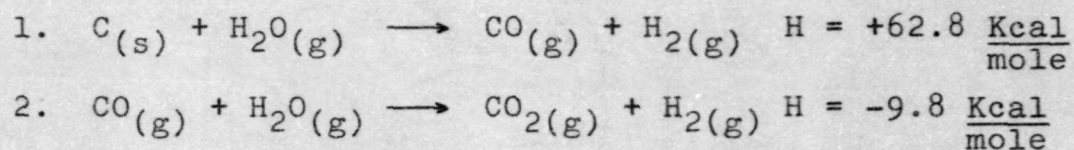
In the United States, during the 1850's, infant refineries emerged in the Appalachian and Ohio River regions producing oil and illuminating gas from shale. (34) When it was estimated that shales in both the eastern and western United States contained over a trillion barrels (i.e. 38 U.S. gallons/barrel) of shale oil, many companies began to express an interest in developing these areas. Among them was Union Oil Company, which in 1950, began processing 1100 tons of shale per day to yield  $165 \times 10^3$  litres per day of crude oil based on a grade of 150 litres per ton of shale, (c.f. 38 litres/ton = 10 U.S. gallons/ton) (35) or approximately 39 U.S. gallons per ton of shale. In 1970, in Colorado, Tosco was processing 900 tons/day at a rate of  $135 \times 10^3$  litres per day based on the same grade. Today, commercial developers in Colorado are aiming for production of  $8 \times 10^6$  liters per day or more.

During the early development of the oil shale industry, better retorting methods were sought to obtain higher yields of oil. It was found that by heating shale in a container (retort), the heat would melt the organic matter to form a liquid. When this liquid was heated to a higher temperature, gases would form. These gaseous vapors could be condensed to form oil and combustible gas. (36)

From the turn of the century through the mid 1920's, research and development of the retorting process led to the

use of steam as a means of improving heat transfer to the oil shale. Use of a pumpherton retort enhanced both the oil recovery and the amount of hydrogen in the off gas.

By 1950, the United States Bureau of Mines used hot recycled gas to initially heat the oil shale. In subsequent experiments super-heated steam at atmospheric pressure was utilized instead of the recycled gas. A significant increase in hydrogen gas production with a corresponding decrease in the carbon monoxide content of the off-gas resulted. The process can be described in terms of the water gas shift reactions.



The importance of equation 2 is that it proceeds rapidly in the presence of water vapor and hot retorted oil shale within a "Royster" retort. (37)

Two modern retorting processes which are currently being developed commercially are:

1. The Hytort process and
2. The Parahoprocess.

The Hytort process was first initiated in the early 1970's by the Institute of Gas Technology as a method for producing synthetic natural gas from the oil shale in the western United States. (38) Hytort's commercial development gained impetus when the feasibility of its application to eastern Devonian shale became known.

The Hytort process involves the direct hydrogenation of the shale oil under controlled heating and elevated pressures. The conversion rates of organic carbon are as follows:

1. 95% conversion for the western oil shale
2. 90% conversion of the eastern oil shale

The products of the Hytort Process, whether synthetic natural gas or syncrude, depend on the operating conditions. Also, Hytort shale oils compared with shale oil produced by thermal methods using the same Devonian shales have a low pour point and are pumpable in a raw state. The reason for upgrading Hytort shale oil is simply to remove the nitrogen content. Table 1 and Table 2 show the results of tests done on Devonian shales under oil-producing and gas-producing conditions, respectively. (39)

The Paraho Process utilizes a combination of indirect and direct heating of eastern oil shale and recovers energy by the direct combustion of the organic carbon in the retorted shale. This combination mode has two advantages:

1. It has an excellent efficiency in recovering all of the heat of combustion of the organic carbon; and
2. The combustion of this organic carbon burns the benza alpha pyrenes which are carcinogenic. (40)

It may be added that both the Hytort Process and the Paraho Process give better conversion yields than the conventional Fischer assay technique, which will now be discussed.

The Fischer assay technique has been utilized by the United States Bureau of Mines in order to measure product

TABLE 1

Results of Tests on Devonian Shales Under Oil-Producing Conditions

Shale Unit Tested	Bench-Scale Tests		Process Development Unit Tests			
	Sunbury	New Albany	Sunbury		New Albany	
			Stage 1	Stage 2	Stage 1	Stage 2
Reactor Pressure, psia	523	522	419	1382	423	1455
Average Shale Temperature, °F	1180	1288	662	608		
Maximum Temperature, °F	1296	1503	807	1461	804	1498
Shale Space Velocity lb/ft <sup>3</sup> -hr	94	82	110	109	121	119
Shale Mass Rate lb/ft <sup>2</sup> -hr	1089	1065	1100	1086	1210	1195
Organic Carbon Distribution, % Gaseous Hydrocarbons <sup>a</sup>	16	28	5	22	3	21 <sup>c</sup>
Shale Oil <sup>a</sup>	58 <sup>b</sup>	51	11	31	7	53
Spent Shale	26	16	27	24	24	24
Total	100	95	96	108	108	108
Oil Properties <sup>d</sup>			Stage 1+2		Stage 1+2	
C/H Weight Ratio	8.3	8.9	8.8		8.9	
Sulfur Content, wt %	1.8	1.6	1.4		1.1	
Nitrogen Content, wt %	1.6	1.9	1.5		1.9	
API Gravity	19.0	13.3	12.2		12.5	
Pour Point, °F	-35	n.d.	-3		-25	
Viscosity, SSU at 100°F	n.d.	n.d.	198		160	

<sup>a</sup>Total distribution for PDU tests is the sum of Stage 1 and Stage 2 distributions.

<sup>b</sup>Adjusted to give 100% carbon balance.

<sup>c</sup>Excluding CO<sub>2</sub> methanation reactions.

<sup>d</sup>Stage 1 and Stage 2 oils combined for PDU oil analysis.

TABLE 2

Results of Tests on Devonian Shales under Gas-Producing Conditions

Shale Unit Tested	Bench-Scale Unit Tests		Process Development Unit Tests			
	New Albany	Chattanooga <sup>c</sup>	Sunbury		New Albany	
			Stage 1	Stage 2	Stage 1	Stage 2
Reactor Pressure, psia	508	533	422		425	
Average Shale Temperature, °F	1415	1370	445	1420	639	1166
Maximum Temperature, °F	1550	1492	804	1498	888	1219
Shale Space Velocity, lb/ft <sup>3</sup> -hr	79	83	126	124	134	132
Shale Mass Rate, lb/ft <sup>2</sup> -hr	1018	990	1260	1244	1340	1319
Organic Carbon Distribution, %						
Gaseous Hydrocarbons <sup>a</sup>	44	39	4	22	4	18
Shale Oil <sup>a</sup>	25	40	7	12	16	9b
Spent Shale	<u>20</u>	<u>21</u>	<u>47</u>		<u>41</u>	
	89	100	92		88	

<sup>a</sup>Total distribution for PDU tests is the sum of Stage 1 and Stage 2 distributions.

<sup>b</sup>Low due to some liquid loss.

<sup>c</sup>Tennessee shale. Other Shales from Kentucky.

yields from oil shale. It requires that a sample be heated in a retort vessel at a rate of  $12^{\circ}\text{C}$ . per minute until a final temperature of  $500^{\circ}\text{C}$  is reached. This temperature is maintained for 20 minutes and yields of oil and water are measured. Figure 2 shows a modified Fischer assay apparatus. <sup>(41)</sup>

In order to understand how oil is produced from the pyrolysis of oil shale, one must look at the structure of the kerogen that is contained within the shale rock. Kerogen is a complex polymer of high molecular weight formed from the decay of marine organisms and plants. These large polymer units are cross linked with shorter bridge chains. Together these chains form a matrix of many hydrocarbons that are both aromatic and aliphatic in nature.

As the temperature rises to approximately  $450^{\circ}\text{C}$ , the cross linked bridges between the large polymer units begin to break first. The decomposition of these shorter chains is called primary cracking. As the temperature rises, fragmentation of the large polymer units also occurs. The fragmentation of these units is called secondary cracking. When cracking occurs, free radicals form and react with other combined hydrogen to form oils. (See Figure 3).

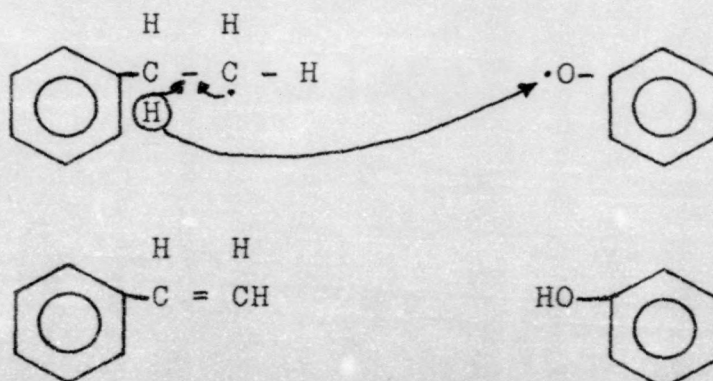


FIGURE 3

Free Radicals Combining with Combined Hydrogen to Form Oils

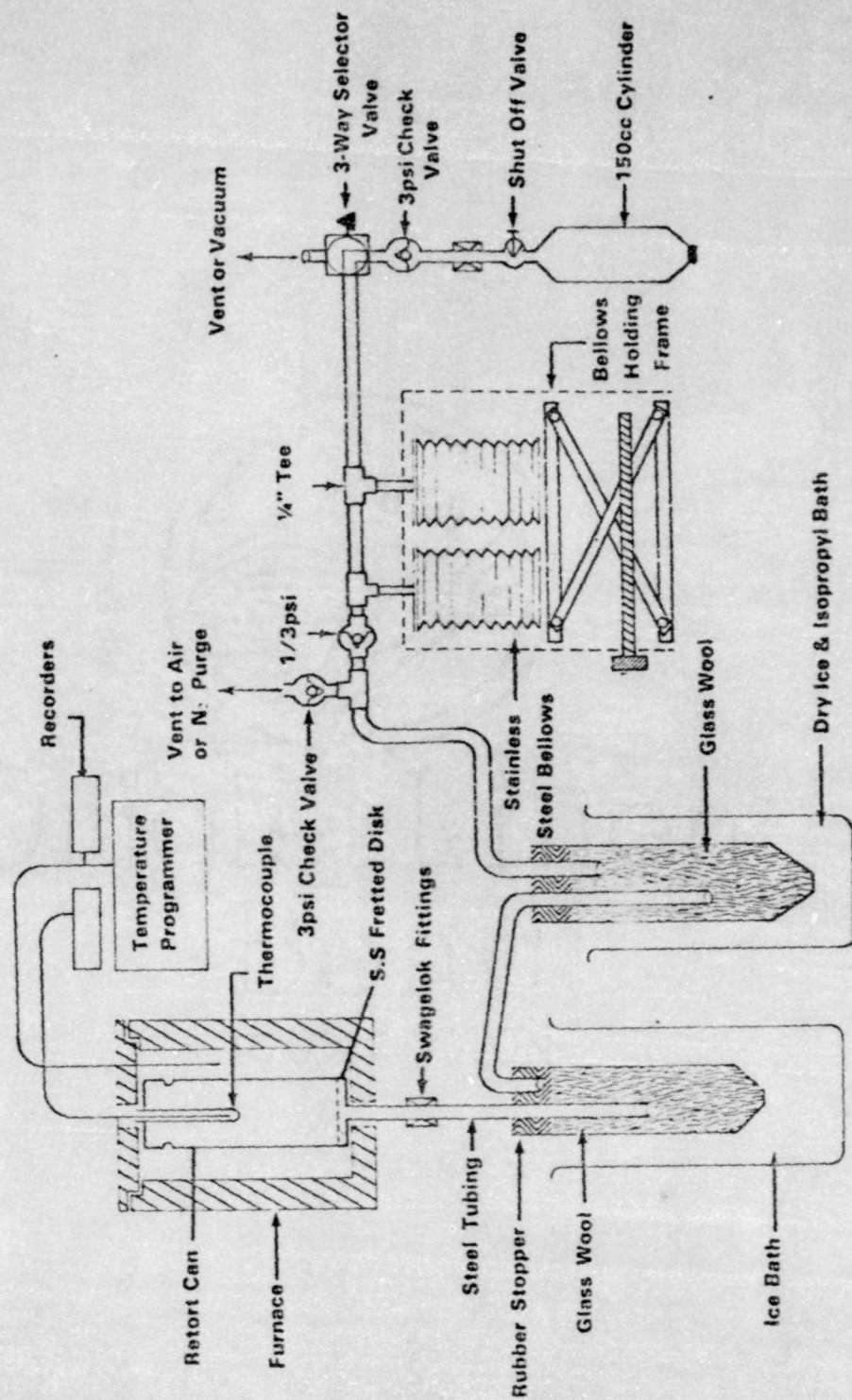


FIGURE 2. A Modified Fischer-Assay Apparatus

As more free radicals are produced the amount of combined hydrogen declines. When this happens two things can occur:

1. Larger molecules can disproportionate as illustrated below:

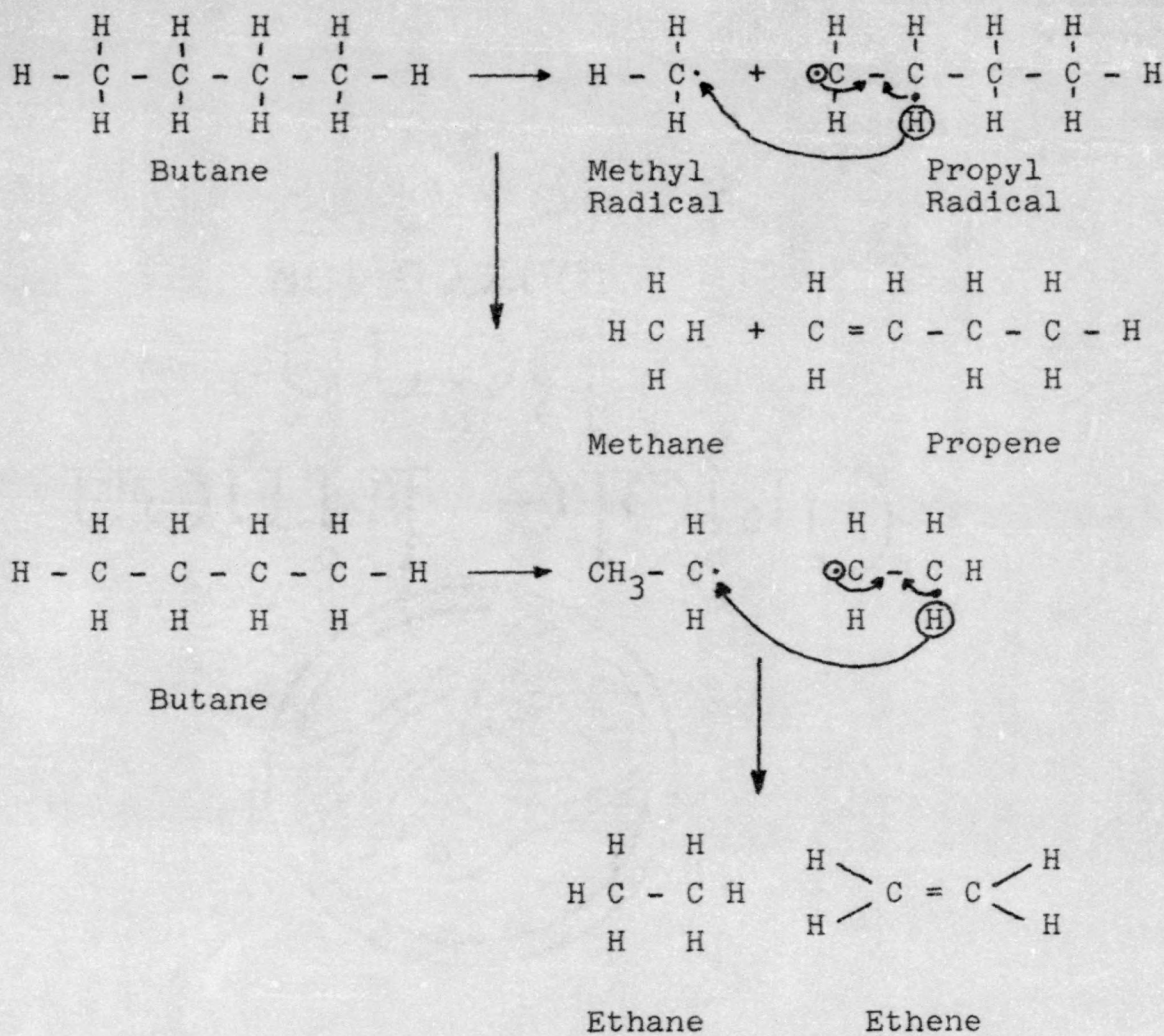


FIGURE 4

Disproportionation of Larger Molecules

2. Free radicals can combine to form Char or Coke. This process is called carbonization or coking and is illustrated by the following mechanism.

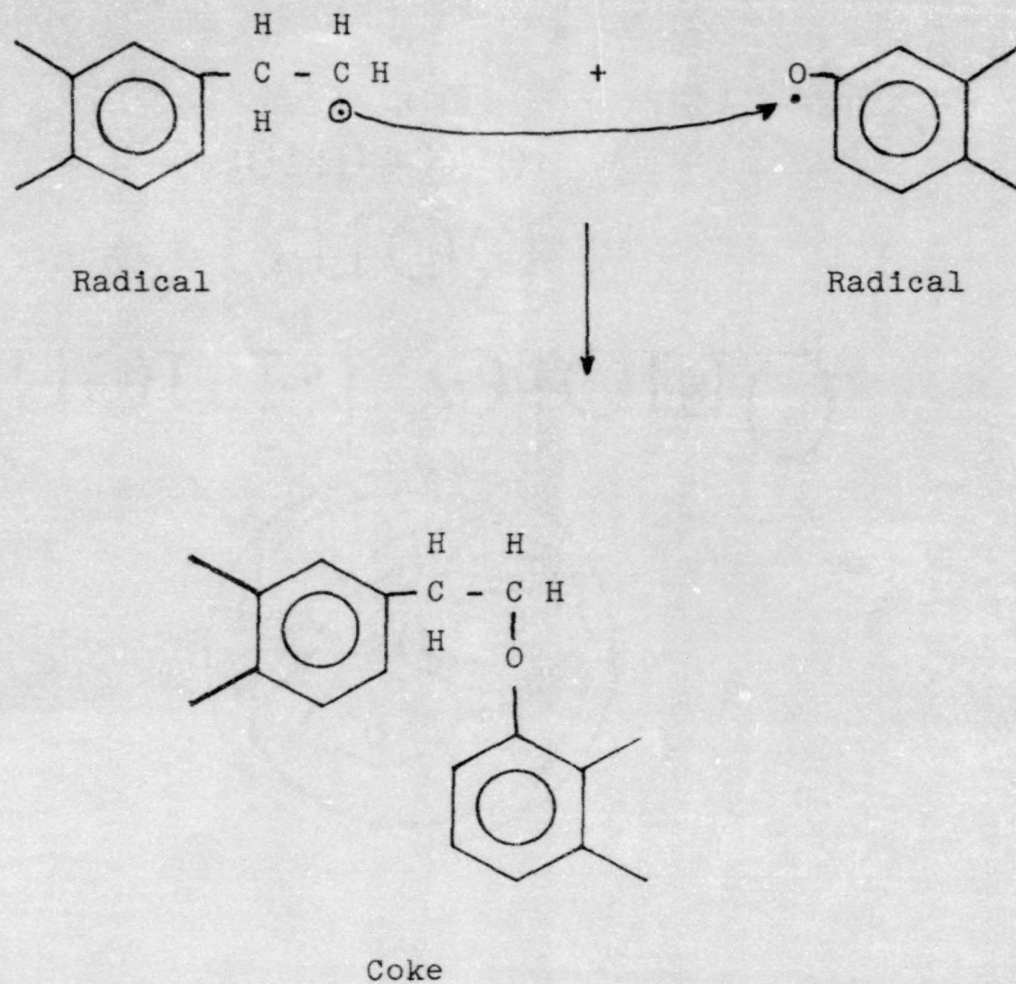


FIGURE 5

Free Radicals Combining to Form Char or Coke

Economic production of shale oil requires optimum oil formation and minimum coke formation. Many of the eastern oil shales are "hydrogen limited" in terms of oil production. Techniques such as hydroretorting successfully enhance the oil yield from the hydrogen deficient eastern oil shales.

Analytical pyrolysis is a technique which can closely approximate Fischer assay conditions with one additional feature: the heating rate and ceiling temperature can be rigidly controlled. With the use of pyrolysis-gas chromatography, a sample can be pyrolyzed with very linear and rapid heating rates while restricting the ceiling temperatures to a pre-determined value. (42)

Presently, there are numerous applications of the analytical pyrolysis-gas chromatograph (AP/GC) technique. For example, in the pyrolysis of coal, rapid heating rates prevent significant decomposition of coal while it is being heated. The sample of coal can then be pyrolyzed at a constant temperature which gives higher volatile yields than can be obtained by using other experimental techniques. Conversely, lower heating rates give lower volatile yields due to the cross linking of coal which prevents material from escaping in the pyrolyzate. (43)

C.S. Giam et al, state that the AP/GC technique can be used to "screen" certain organic wastes such as cotton gin wastes and bovine manure as potential sources of hydrocarbons for fuel and for chemical use. (44)

Levy has also demonstrated the reproducibility of AP/GC in characterizing automotive paints. (45) In addition, Chemical

Data Systems has used AP/GC to obtain analytical data on wood and bark which presently cannot be obtained in any other way. (46)

Another versatile application of AP/GC is the thermal distillation pyrolysis on petroleum source rock and polluted marine sediments using the apparatus shown in Figure 6. (47) In this technique 0.5-50 mg samples of wet sediment are placed in a quartz tube which in turn is placed in a pyroprobe. The pyroprobe is then programmed from 100 to 800°C at a rate of 20°/min. Two well separated peaks, P<sub>1</sub> and P<sub>2</sub>, are observed on the pyrogram. P<sub>1</sub> contains all unchanged hydrocarbons which evolve between 100 to 150°C and is very sharp compared to the pyrolysis peak, P<sub>2</sub>, which contains cracked hydrocarbons that evolve between 650 to 800°C. If P<sub>2</sub> is a result of the thermal decomposition of the kerogen in petroleum source rocks, then the area of P<sub>2</sub> might be a measure of the petroleum generation capacity of the rock. Also, if P<sub>1</sub> increases as the depth of the rock increases due to the lipid hydrocarbons, then a quantitative relationship for petroleum generation called the production index (P.I.) can be expressed by the following equation: (48)

$$P.I. = \frac{P_1}{P_1 + P_2}$$

Whelan et al., have done studies on La Luna and Posidonien shales from Columbia, South America, and Western Europe. Figure 7 (49) and Figure 8 (50) show the P<sub>1</sub> peaks of the capillary GC analyses on these two shales, respectively. The sharp peaks show the n-alkanes while the lower

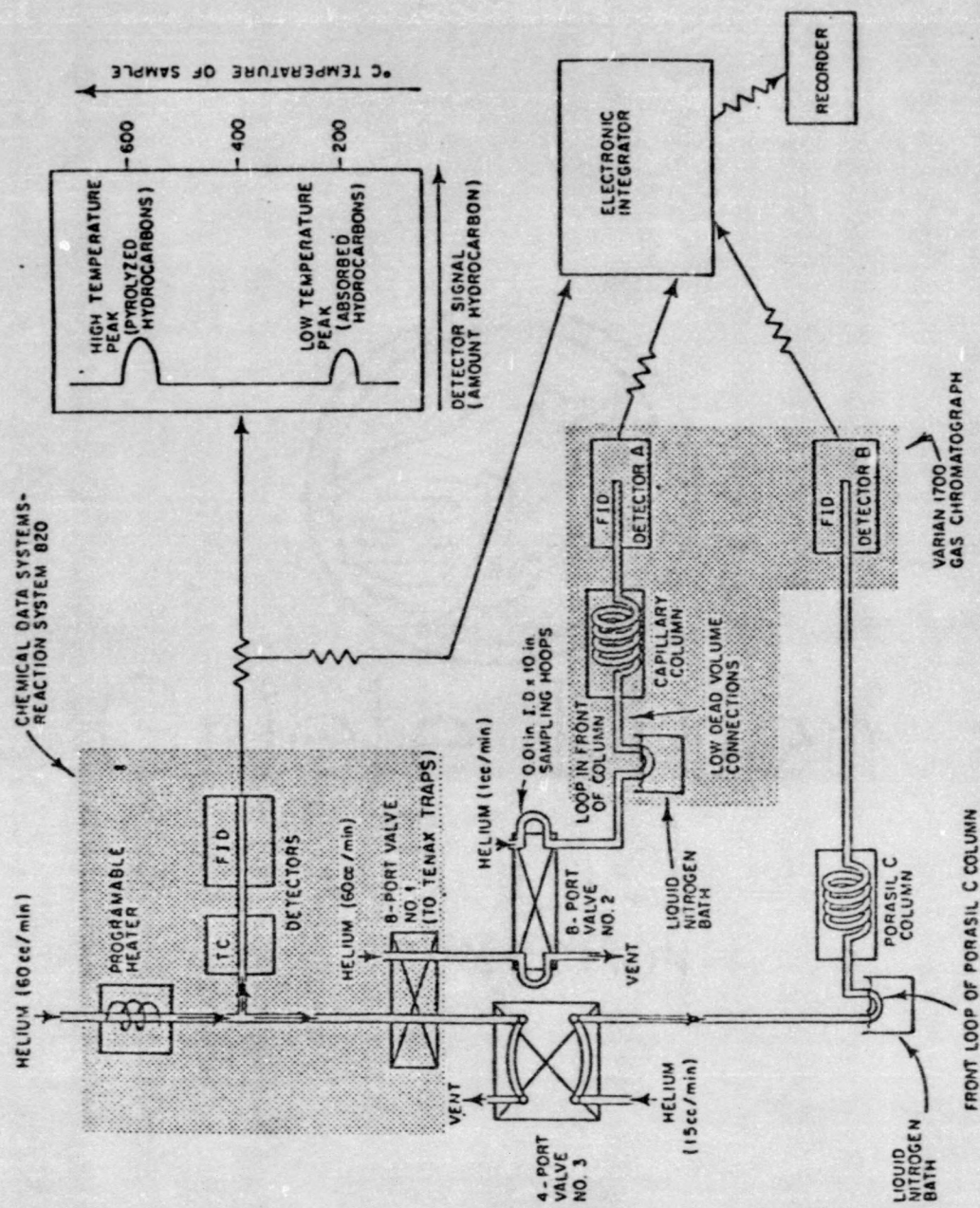
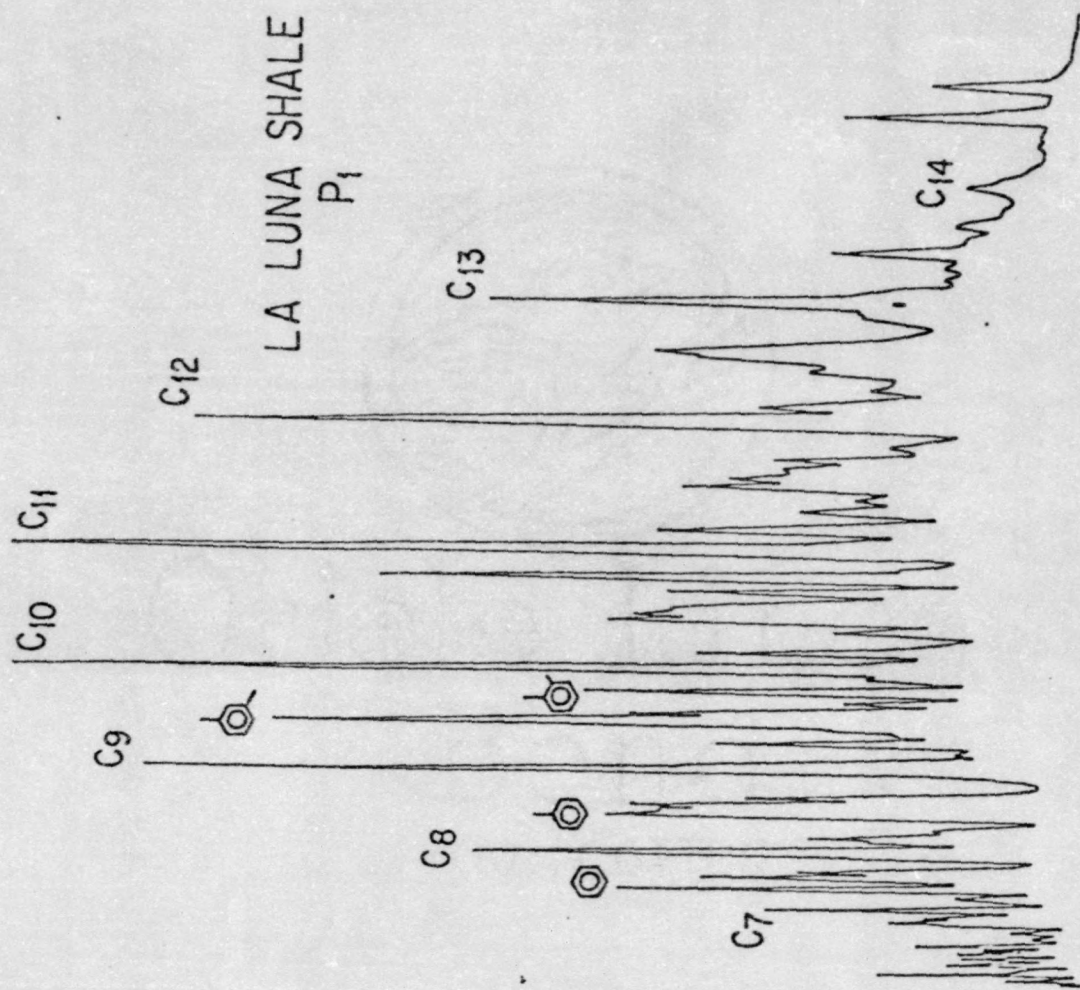
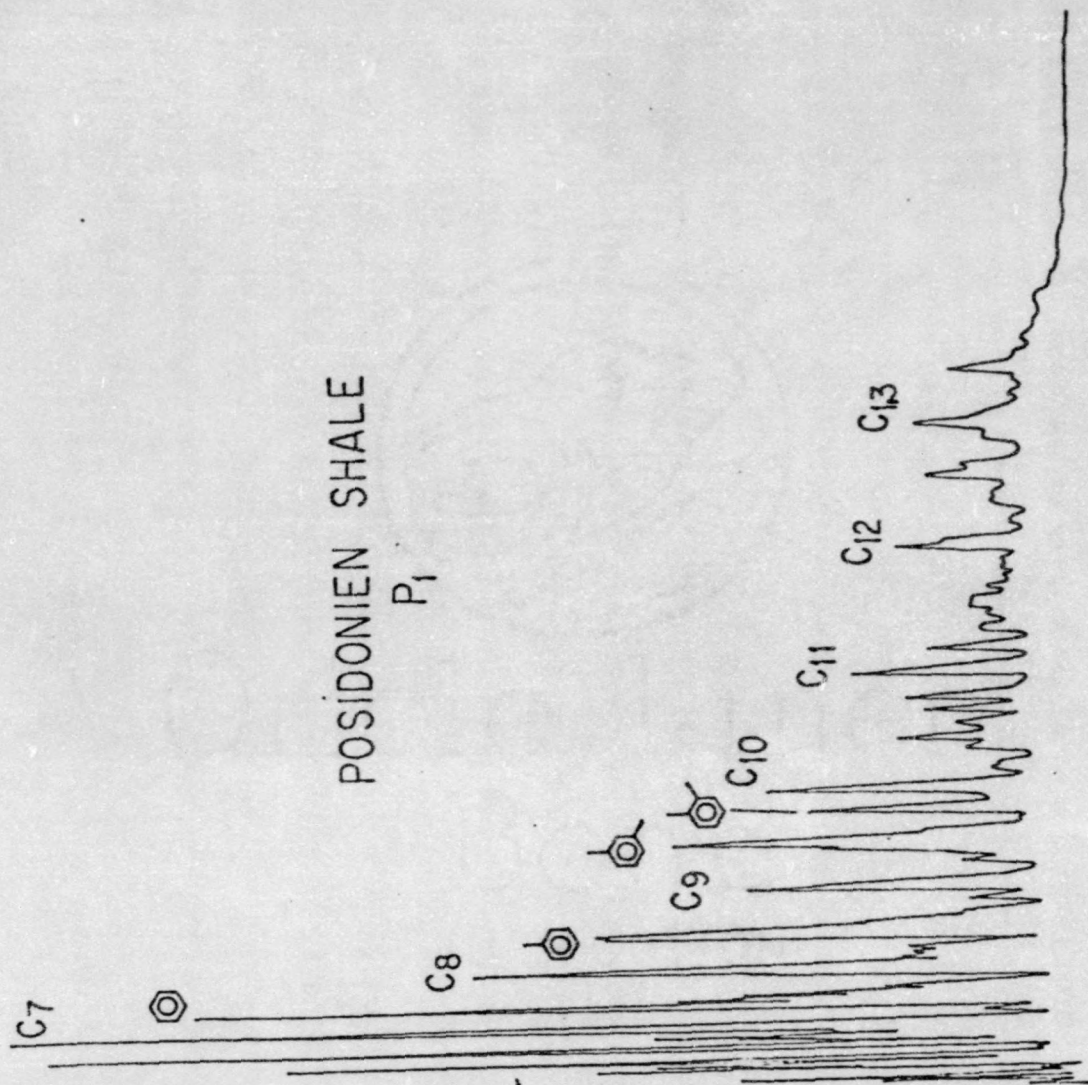


FIGURE 6. Chemical Data Systems 820 Reaction System

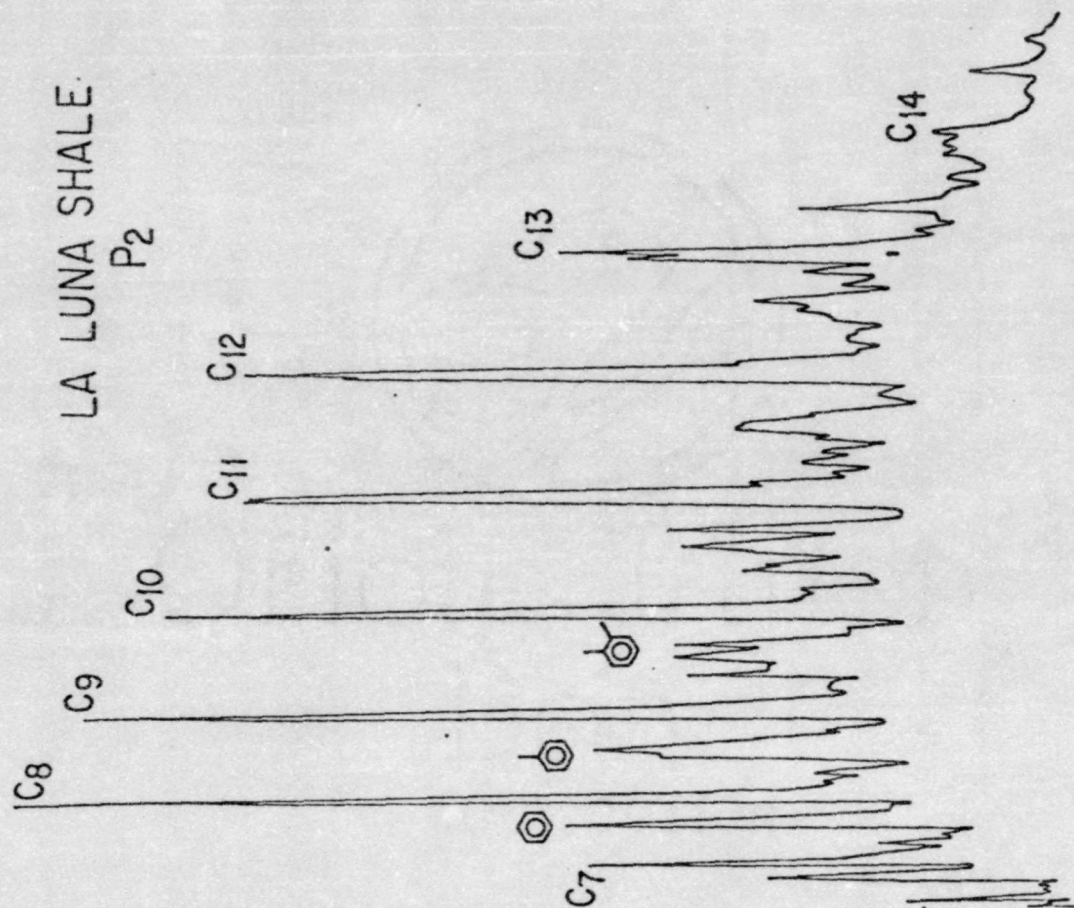
FIGURE 7. Pyrogram of La Luna Shale P<sub>1</sub>

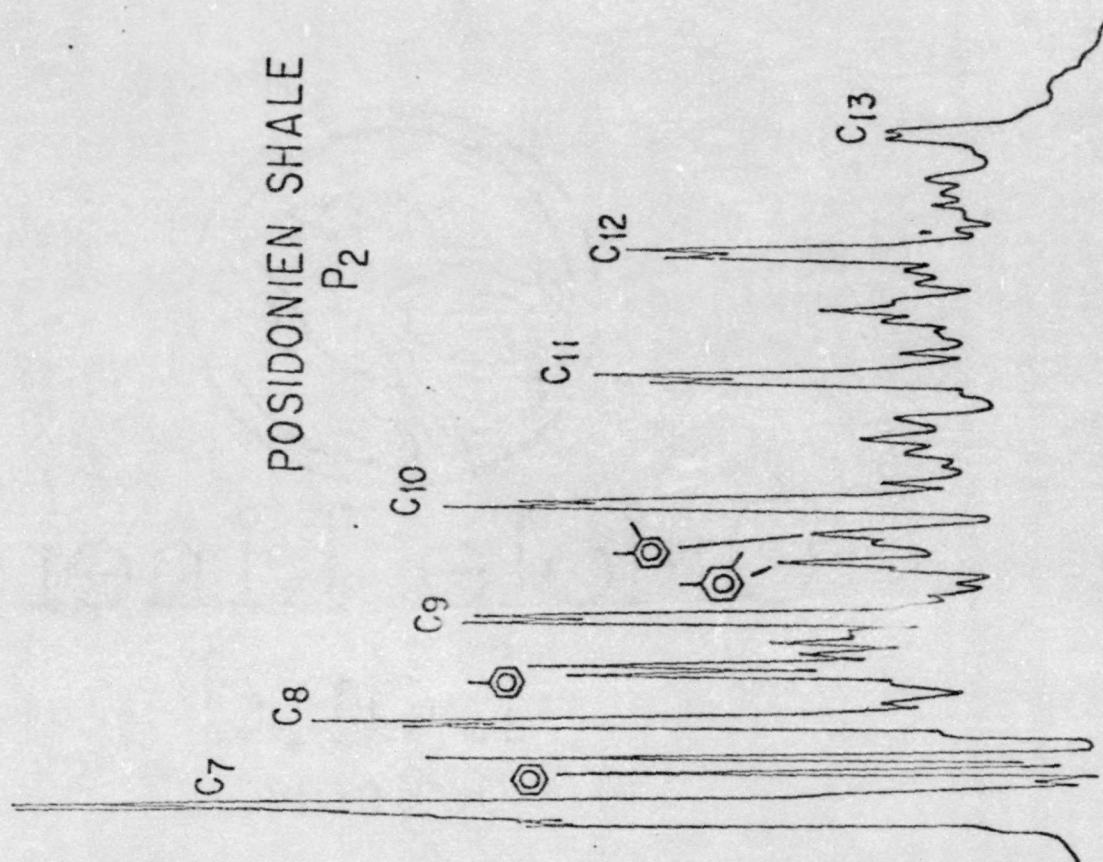
FIGURE 8. Pyrogram of Posidonien Shale P<sub>1</sub>

unresolved peaks occur because of the aromatic nature of the petroleum product. By correlating the changes in the nature, maturity and migration of the kerogen, with depth of the source rock, it is possible to predict the nature of the petroleum product. For example, lighter hydrocarbons occur in greater depths of more mature rocks within a kerogen that has not moved; and biodegraded oil will retain the unresolved peaks in a pyrogram while the sharp peaks of the n-alkenes disappear.

Figures 9<sup>(50)</sup> and Figures 10<sup>(52)</sup> show the P<sub>2</sub> peaks of the capillary G.C. analyses for the La Luna and Posidonien shales. However, due to the aromatization, unsaturation and condensation of these released molecules, interpretation of the resulting pyrograms must be done with great care. For example, the well resolved double peaks in both figures represent alkane plus alkene of the same carbon number which are generated from the kerogen matrix by the thermal cracking process. But due to the reproducibility of the patterns obtained from the pyrolytic products, these characteristics may be used in finger printing the kerogens from which the petroleum is derived. There are very few other methods besides AP/GC analysis that can examine these extremely complex substances.

The purpose of our investigation was to study the effects of ceiling temperature, heating rate (ramp) and pyrolysis interval on the product yield and distribution from two eastern oil shales by the employment of the analytical pyrolysis (pyrolysis-gas Chromatograph Technique).

FIGURE 9. Pyrogram of La Luna Shale P<sub>2</sub>

FIGURE 10. Pyrogram of Posidonien Shale P<sub>2</sub>

## EXPERIMENTAL

### Oil Shales

Two eastern oil shale samples were used in this study. These were noted as Cleveland (of the Devonian Age) and Sunbury (of the Mississippian Age) from Lewis County in northeastern Kentucky. Fischer assay work shows that oil yields for Cleveland are 14.0 gal/ton and 16.0 gal/ton for Sunbury. Specimens of each shale used in this study were in the 60/100, 30/60, -30, and -100, mesh range. The elemental and proximate analysis of the raw shale shown in the table below was prepared by the Institute for Mining and Minerals Research Laboratory in Lexington, Kentucky.

TABLE 3  
Analysis of the Raw Shale

<u>Elemental Analysis - Fischer Assay</u>				
<u>Shale</u>	<u>% Carbon</u>	<u>% Hydrogen</u>	<u>% Nitrogen</u>	<u>Oil Yield</u>
Sunbury	16.3	1.9	0.6	16.4 gal/ton
Cleveland	14.7	1.9	0.55	14.0 gal/ton

<u>Thermogravimetric Analysis</u>				
<u>Shale</u>	<u>% Moisture</u>	<u>% Volatile Matter</u>	<u>% Fixed Carbon</u>	<u>% Ash</u>
Sunbury	0.90	15.6	7.10	---
Cleveland	2.3	15.1	6.6	---

### Instrumentation

A Chemical Data Systems Model 100 pyroprobe, a Model 382 extended pyroprobe, and a Model 310 concentrator were interfaced with a Varian Model 3700 gas chromatograph (dual flame ionization detectors) and a Laboratory Data Control Model 308 computing integrator. This enabled the oil shale samples to be pyrolyzed at the ceiling temperatures ranging from 200°C to 1000°C. Temperature ramps (heating rates) from 5°C per minute through 500°C per second can be used for intervals of up to 240 minutes.

Pyrograms were recorded by a Varian Aerograph Model 20 recorder, and peaks were electronically integrated in order to obtain the relative amounts of material in the high volatile (low molecular weight) and low volatile (high molecular weight) regions of the pyrogram for each individual sample.

A 50 cm x 1/8 inch stainless steel 5% OV-101 column was used. The flow rate of carrier gas (nitrogen) was approximately 40 ml per minute. The interface unit was regulated at 200°C and the 310 concentrator traps A and B were pulse heated to 250°C. Injector temperature was set at 270°C and sensitivity was  $10^{-10}$  amps/mv.

### Procedure

High purity quartz tubes 2.4 mm od x 2.5 cm long were loosely fitted with quartz wool plugs to ensure the evolution of the volatiles from the samples. The tubes were heated to 1000°C for 10 seconds in order to burn away any organic

oils which might adhere on the tubes through handling. The tubes were weighed on a Mettler Model H-20T analytical balance. Approximately 4-5 mg of the 60/100 mesh samples were introduced into the clean quartz tubes. Care was taken not to contaminate them during handling. These were weighed again, and the actual weight of the sample found by difference.

The tubes were placed inside the coil of the CDS pyroprobe heater unit and placed inside the interface unit attached to the injection port of the gas chromatograph. The desorber button was then pushed and the interface unit containing the tube allowed to heat to 200°C. The sample in the tube was allowed to equilibrate for 10 minutes. After 10 minutes, the reset button on the Model 382 extended pyroprobe (to set all times) and the run button on the 100 pyroprobe (to pyrolyze the sample at the prescribed ramp, ceiling temperature and interval) were depressed.

The sample reached the ceiling temperature and volatiles were allowed to collect into either Trap A or Trap B of the Model 310 Concentrator. The sample was held at the ceiling temperature for the duration of the interval, after which the laboratory Data Control Model 308 Computing Integrator was zeroed. This was done by pushing the manual button on the integrator and setting the Bridge of the Varian Model 3700 to zero. The upper button of the Detector Mode was depressed, and the zero knob was adjusted until zero counts were observed by the print out of the integrator. This was done three to four minutes before the sixty minute pyrolysis interval was completed.

When the interval light on the extended pyroprobe went out, the valve of either Trap A or Trap B was opened to allow the volatiles to be swept into the GC column and the trap heated to a maximum of 250°C.

The amount of eluate from the volatiles (i.e. low molecular weight) was detected by the gas chromatograph and the data was stored in the integrator where counts were printed out at regular one minute intervals. Simultaneously, the detector signal was recorded by the Varian Aerograph Model 20 recorder in the form of a pyrogram. The pyrogram recorded the different fractions of the constituents contained in the sample, from which relative product ratios for the high volatile and low volatile products were determined.

When the Trap Heater was activated the following program began:

1. The column temperature was held at 60°C for 10 minutes (isothermal) after which the column temperature rose at the rate of 20°C/min. to a maximum of 250°C where it was held for 30 minutes. The time for the program was exactly 49.5 minutes, and the total time for the complete run was 119.5 minutes or approximately two hours. For any given set of parameters (e.g. ceiling temperature, ramp and interval) replicates of 8 to 10 runs were made in order to ensure that the data was representative of the trends found in the statistical analysis. Average values and standard deviations were calculated.

The resulting pyrogram was divided into two regions as shown in Figure 11. The high volatile fraction was recorded

GC Column Programmed  
at 20C/minute to 250°C-hold

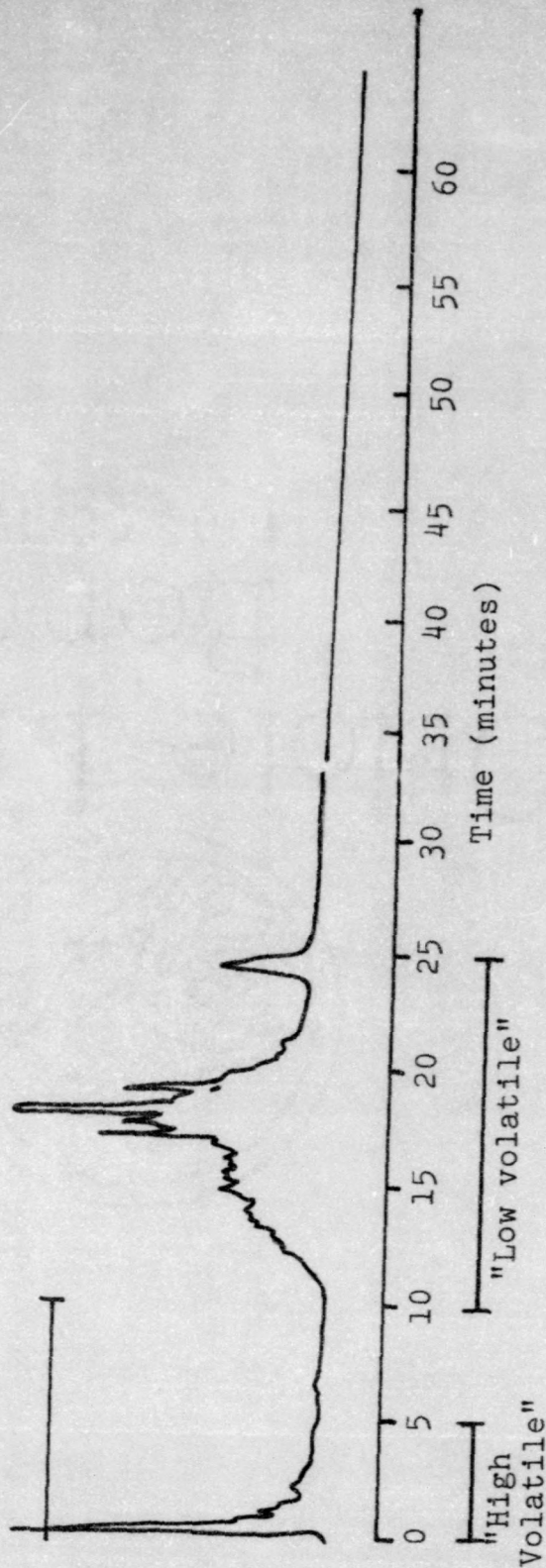


FIGURE 11. Typical Pyrogram Showing High Volatile and Low Volatile Fractions.

from 1-5 minutes; the corresponding counts on the integrator were recorded. The low volatile fraction was observed between the 11th and 26th minutes of the program and again the corresponding counts were recorded. The counts for both fractions were totaled and were divided by the weight of the sample to obtain the counts per milligram. The percentages of both the high and low volatile fractions were found by dividing the counts representing that fraction by the total number of counts and multiplying by 100.

The spent shale samples were weighed on the Mettler H-20T and the weight loss found by difference. The percentage weight loss was found by comparing the weight loss to the total weight of the sample  $\times 100$ . The weight loss for each sample was due to the organic material being volatilized, and by the loss of water, hydrogen, hydrogen sulfide, carbon dioxide and other materials not recorded by the pyrogram. The percentages of high volatile, weight loss and counts/mg were tabulated. Average values and standard deviations were calculated.

Table 3 shows carbon-hydrogen-nitrogen and thermogravimetric analysis that was performed on the spent shale samples by the Institute for Mining and Minerals Research, Lexington, Kentucky. The differences in carbon content before and after pyrolysis as well as the differences between the volatile matter in the raw and spent shale can be used as estimates or measures of the total product yield.

#### Pyroprobe Calibration

A 58.48 mg sample of Kraton 1107 co-polymer (Shell

Chemical Co., Houston, Texas) was dissolved in benzene in a 5 mL volumetric flask. A 2 microliter sample of the solution was withdrawn by a syringe and injected into a quartz wool plug inside a 2.4 mm od x 2.5 cm long quartz tube. The tube was placed inside the platinum coil of the Pyroprobe and placed in the interface unit.

The column temperature was set at 250°C and the sample in the interface unit allowed to equilibrate for 8 minutes to drive off the benzene (solvent). After 8 minutes the column temperature was lowered to 200°C and the gas chromatograph zeroed. The sample was then pyrolyzed at the 650°C and 750°C set points at a rate of 500°C/second for a pyrolysis interval of 10 seconds. Attenuations were set at 128X for isoprene, 64X between isoprene and styrene and 16X for the remainder of the chromatogram. In addition, flow rates through the column (4 ft x 1/8 inch stainless 80/100 Poropak Q) were adjusted so that the isoprene peak eluted at 6.5 minutes and the dipentene at 10.3 minutes.

After the chromatograms are recorded, the peak areas of the isoprene peak and the dipentene peak are calculated from the formula below.

$$\text{Peak Area} = \text{Peak Height} \times \text{Peak Width at } 1/2 \text{ Peak Height}$$

The isoprene area is then divided by the dipentene area to determine the ratio. Levy and Walker have shown that the isoprene/dipentene ratio is temperature sensitive and may be used to calibrate pyrolysis equipment.<sup>(53,54)</sup> The Levy-Walker

calibration curve is shown in Figure 12. The results of the calibration experiments are given in Table 4.

TABLE 4

<u>Run No.</u>	<u>Set Temp.</u>	<u>Isoprene/ Dipentene</u>	<u>Equivalent Temp.</u>	<u>Average Temp.</u>
1	650°C	1.19	594	
2	650°C	1.51	628	
3	650°C	1.53	629	
4	650°C	1.59	635	
				622 ± 16°C
1	750°C	2.58	703	
2	750°C	2.48	697	
3	750°C	3.20	748	
4	750°C	2.93	728	
				719 ± 20°C
		Solid Polymer		
1	650°C	0.96	589	
2	650°C	1.20	605	
3	650°C	0.86	582	
4	650°C	1.03	596	
				593 ± 9°C
1	750°C	1.95	660	
2	750°C	1.80	650	
3	750°C	1.95	660	
4	750°C	1.85	655	
				656 ± 4°C

As is shown from the above table, the ratios of both the solid co-polymer and solution gave lower equivalent temperatures than the set-point value.

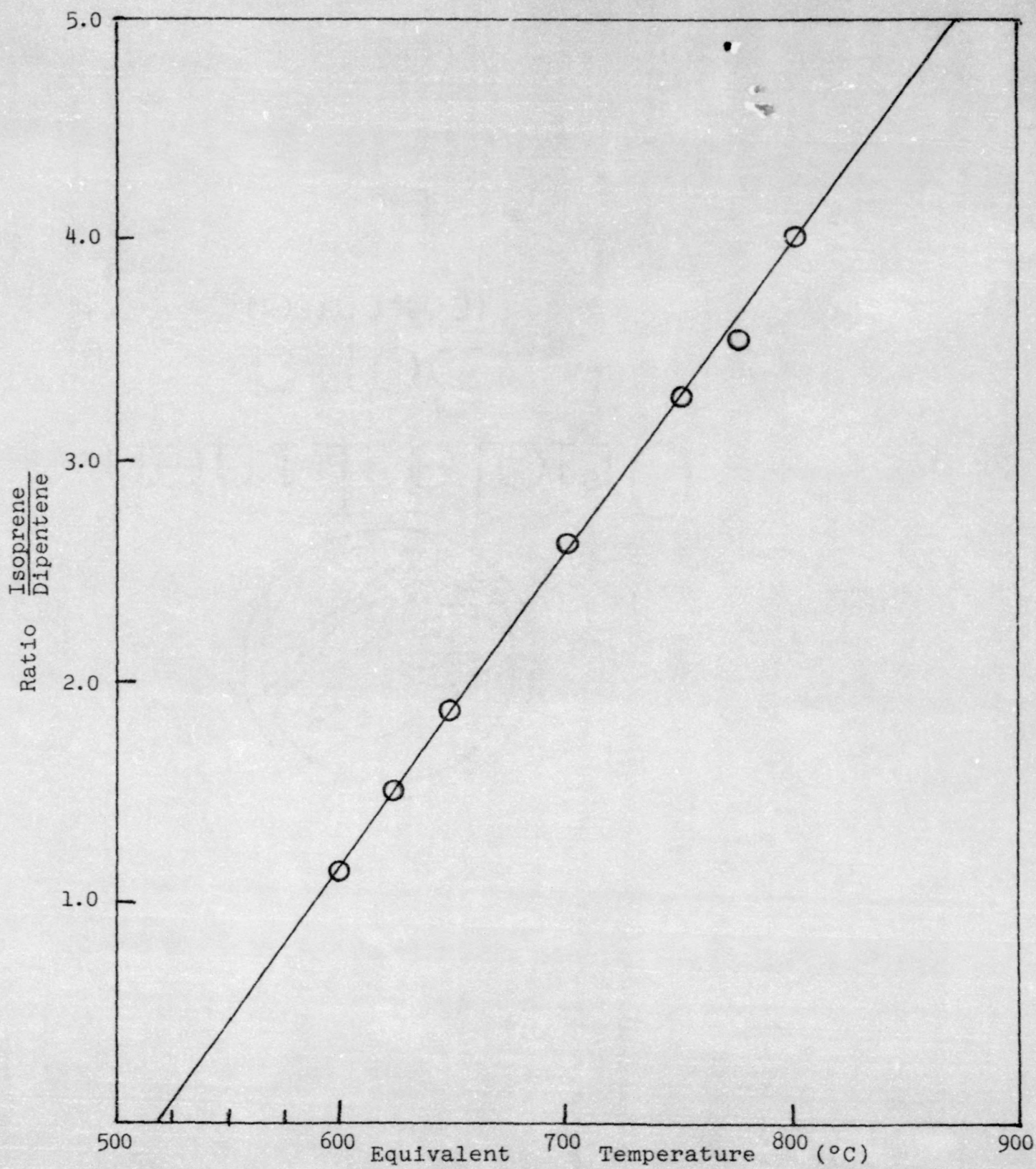


FIGURE 12. The Levy-Walker Molecular Thermometer Calibration Curve for Kraton 1107 Polymer

It was noted also that when runs at 550°C, 500°C and 450°C respectively with solid co-polymer were tried, the equivalent temperatures were all higher than the respective ceiling temperatures. This may well be due to the sample not being completely pyrolyzed. There is likely some threshold temperature below which efficient pyrolysis of the co-polymer does not occur. Indeed, at the end of the 450°C run it was observed that the co-polymer was fused to the quartz tube and did not completely pyrolyze. This effect was also observed for the 500°C and 550°C ceiling temperatures. Also, it was noted that when the sample did not pyrolyze completely, the isoprene peaks were reduced and no styrene peaks were shown at 6-7 minutes. This alters the Isoprene:Dipentene ratios greatly because there was very little Isoprene detected on the pyrogram.

Table 4 indicates that there is a lower equivalent temperature for the solid co-polymer than for the solution. This may be due to the less efficient heat transfer inside the quartz tube with the solid co-polymer. However, for the solid and solution, the temperatures experienced by both are probably the more accurate indicators of ceiling temperature that the oil shale experiences during the 10 second pyrolysis interval. It should also be noted that the longer the pyrolysis interval, the closer the internal temperature should be to the set-point ceiling temperature on the pyroprobe.

## RESULTS

Before beginning a study of the effect of heating rates and mesh size on the pyrolysis yield and product distribution from eastern oil shale, it was necessary to check the performance of the Chemical Data Systems Model 310 Concentrator and its associated "purge-traps" system. Since data was already available for the pyrolysis of Sunbury shale at a ramp of 500°C/second for 20 seconds at 550°C, 650°C and 750°C, these experiments were repeated under the same operating conditions with the Model 310 Concentrator in use. The experimental results for the 550°C, 650°C and 750°C ceiling temperatures are given in Tables 5, 6 and 7 respectively.

TABLE 5  
Sunbury Shale

Sample #	Sample Weight	% H.V.	% L.V.	% Wt. Loss	C/M
1) 110	4.92	24.5	75.5	12.4	71.6
2) 111	3.83	27.2	72.8	16.7	80.8
3) 112	3.68	25.6	74.4	13.3	61.3
4) 114	3.33	29.5	70.5	9	52.3
5) 115	4.30	32.0	68.0	...	58.6
6) 116	4.35	30.9	69.1	...	61.5
Mean 0	4.07	28.2	71.7	12.9	64.4
S.D. 0	0	2.85	2.73	2.74	9.30

Ceiling Temperature = 550°C  
 Heating Rate = 500°C/sec  
 Attenuation = 64  
 Heating Interval = 20 sec  
 Mesh Size = 60/100

TABLE 6  
Sunbury Shale

Sample #	Sample Weight	% H.V.	% L.V.	% Wt. Loss	C/M
1) 102	4.08	32.9	67.1	14.46	119.4
2) 103	5.62	28.4	71.6	15.12	105.6
3) 104	3.11	25.2	74.8	...	120.1
4) 106	4.94	32.6	67.4	12.55	106.0
5) 107	3.47	30.6	69.4	...	90.1
6) 108	4.95	32.4	67.6	15.96	121.0
7) 109	3.36	27.2	72.8	12.20	93.5
Mean	4.22	29.9	70.1	14.06	108.
S.D.		2.79	2.79	1.45	11.9

Ceiling Temperature = 650°C  
 Heating Rate = 500°C/sec  
 Attenuation = 64  
 Heating Interval = 20 sec  
 Mesh Size = 60/100

TABLE 7  
Sunbury Shale

Sample #	Sample Weight	% H.V.	% L.V.	% Wt. Loss	C/M
1) 90	3.15	36.7	63.3	15.87	130.9
2) 91	5.57	35.7	64.3	17.95	113.8
3) 92	3.29	33.4	66.4	10.64	139.9
4) 93	3.01	32.9	67.1	20.60	142.5
Mean 0	3.76	34.7	65.3	16.27	131.8
S.D. 0	...	1.58	1.54	3.655	11.24

Ceiling Temperature = 750°C  
 Heating Rate = 500°C/sec  
 Attenuation = 64  
 Heating Interval = 20 sec  
 Mesh Size = 60/100

These results correlated well with the "straight run" pyrolysis experiments and followed the same trends. The distillate fraction analyzed separately on straight run pyrolysis was trapped and distributed among the low molecular and high molecular weight fractions using the concentrator. With evidence of proper functions of the concentrator assembly, experiments were conducted at a number of different heating rates.

Experiments were first conducted on 60/100 mesh Cleveland and Sunbury shale at heating rates of 10°C per minute. The ceiling temperature was set at 500°C and the total pyrolysis interval set at 60 minutes. This combination of parameters closely approximates Fischer assay conditions. The results of the 10°C per minute ramp for Cleveland and Sunbury shale are given in Tables 8 and 9 respectively.

In order to investigate the effects of increasing heating rate (ramp) on the overall product yield and distribution for these two shales, heating rates of 120°C per minute, 300°C per minute, 100°C per second, and a nonlinear heating rate of approximately 600°C per second were employed.

The experimental results obtained for Cleveland shale at 120°C/minute, 300°C/minute, 100°C/second, and 600°C/second are given in Tables 10 through 13. Likewise, the results for the samples of Sunbury shale at the same series of heating rates is given in Tables 14 through 17.

Samples of both Cleveland and Sunbury shales were weighed after pyrolysis and the percent weight loss determined. Samples show a good deal of variability due to losses from

TABLES 8-17: Experimental Results of Effect of Heating  
Rates Cleveland and Sunbury Shales.

TABLE 8  
Cleveland Shale

Sample #	Sample Weight	% H.V.	% L.V.	% Wt. Loss	C/M
1) 168	5.43	26.15	73.85	10.3	133.1
2) 169	5.39	25.65	74.35	7.24	105.5
3) 170	4.49	27.72	72.28	11.8	129.5
4) 175	3.82	29.02	70.98	11.26	155.6
5) 176	4.04	22.89	77.11	7.67	111.4
6) 177	4.81	31.08	68.92	9.15	110.3
7) 178	5.38	24.51	75.49	12.45	151.1
8) 179	4.72	25.16	74.84	8.47	104.6
9) 180	5.64	26.14	73.86	8.33	93.0
10) 181	4.46	27.96	72.04	12.56	135.3
11) 182	5.46	30.30	69.70	11.72	120.4
Mean	4.87	26.96	73.04	10.09	122.7
S.D.	...	2.39	2.389	1.889	19.06

Ceiling Temperature = 500°C  
 Heating Rate = 10°C/minute  
 Attenuation = 64  
 Heating Interval = 60 min  
 Mesh Size = 60/100

TABLE 9  
Sunbury Shale

Sample #	Sample Weight	% H.V.	% L.V.	% Wt. Loss	C/M
1) 148	5.66	26.18	73.82	12.37	187.4
2) 149	3.95	25.26	74.74	...	186.7
3) 150	4.41	26.64	73.36	13.38	118.6
4) 151	5.27	30.52	69.48	...	148.8
5) 152	4.51	26.89	73.11	10.2	187.7
6) 153	4.35	25.85	74.15	...	130.3
7) 154	4.16	29.10	70.90	10.82	189.9
8) 155	4.13	26.79	73.21	...	149.2
9) 156	4.13	25.73	74.27	10.17	100.8
10) 158	3.53	27.79	72.21	16.71	171.4
11) 159	4.07	29.09	70.91	18.18	157.3
12) 160	4.44	30.90	69.10	...	160.0
13) 161	4.17	29.07	70.92	13.67	163.7
14) 162	4.63	31.90	68.10	13.17	165.3
15) 163	4.37	29.88	70.12	...	218.8
16) 164	5.10	26.33	73.67	14.31	164.5
Mean	4.43	28.00	72.00	13.30	162.6
S.D.	...	2.013	2.016	2.511	28.53

Ceiling Temperature = 500°C  
 Heating Rate = 10°C/min  
 Attenuation = 64

Heating Interval = 60 min  
 Mesh Size = 60/100

TABLE 10

## Cleveland Shale

Sample #	Sample Weight	% H.V.	% L.V.	% Wt. Loss	C/M
1) 204	3.91	31.32	68.67	15.86	61.4
2) 205	5.55	31.67	68.33	13.87	125.1
3) 206	4.37	29.03	70.97	18.31	139.9
4) 207	3.66	27.25	72.75	13.39	137.4
5) 208	3.77	28.60	71.40	14.85	146.1
6) 209	4.93	29.61	70.39	27.99	119.6
7) 210	3.68	28.51	71.49	14.95	149.2
8) 211	5.14	29.47	70.53	16.15	124.5
9) 212	5.48	28.08	71.92	14.23	95.8
Mean	4.50	29.28	70.72	16.62	122.
S.D.		1.362	1.364	4.250	26.4

Ceiling Temperature = 500°C

Heating Rate = 120°C/min

Attenuation = 64

Heating Interval = 60 min

Mesh Size = 60/100

TABLE 11

## Cleveland Shale

Sample #	Sample Weight	% H.V.	% L.V.	% Wt. Loss	C/M
1) 234	4.62	31.00	69.00	11.90	125.6
2) 236	5.22	29.12	70.88	13.27	161.6
3) 237	4.00	30.25	69.75	13.50	141.0
4) 238	3.45	29.65	70.35	13.04	141.2
5) 239	5.62	30.05	69.95	9.96	125.9
6) 240	4.88	28.75	71.25	11.68	124.9
7) 241	5.54	31.31	68.69	11.73	116.6
8) 242	4.92	30.35	69.65	10.77	121.7
9) 243	3.55	28.37	71.63	8.45	124.8
10) 244	4.20	31.29	68.71	15.24	129.0
11) 245	4.25	31.91	68.09	11.76	119.2
Mean	4.59	30.19	69.63	11.94	130.1
S.D.	..	1.085	1.237	1.756	12.43

Ceiling Temperature = 500°C

Heating Rate = 300°C/min

Attenuation = 64

Heating Interval = 60 min

Mesh Size = 30/60

TABLE 12  
Cleveland Shale

Sample #	Sample Weight	% H.V.	% L.V.	% Wt. Loss	C/M
1) 246	4.76	26.73	73.27	10.08	65.5
2) 248	5.56	32.32	67.68	12.23	115.8
3) 249	4.28	26.05	73.95	15.65	146.9
4) 250	3.32	27.94	72.06	17.47	146.9
5) 251	4.68	30.98	69.02	12.39	125.9
6) 252	4.45	29.73	70.27	15.51	122.4
7) 253	3.62	30.86	69.14	12.71	144.8
8) 255	5.35	27.97	72.01	12.15	113.6
Mean	4.50	29.07	70.93	13.52	123
S.D.	...	2.090	2.088	2.275	25.28

Ceiling Temperature = 500°C  
 Heating Rate = 100°C/sec  
 Attenuation = 64  
 Heating Interval = 60 min  
 Mesh Size = 60/100

TABLE 13  
Cleveland Shale

Sample #	Sample Weight	% H.V.	% L.V.	% Wt. Loss	C/M
1) 283	4.03	31.06	68.94	13.65	113.0
2) 284	3.58	23.90	76.10	10.34	125.2
3) 286	4.50	22.66	77.34	9.11	90.6
4) 288	4.03	29.96	70.04	9.18	102.4
5) 289	3.92	27.41	72.59	15.05	120.4
6) 290	4.25	28.65	71.35	12.24	103.9
7) 291	3.35	26.22	73.78	17.01	140.5
8) 292	4.21	26.70	73.30	9.26	116.6
9) 293	4.57	30.40	69.60	13.79	114.8
Mean	4.05	27.44	72.56	12.2	114.2
S.D.	..	2.730	2.730	2.72	13.59

Ceiling Temperature = 500°C  
 Heating Rate = 600°C/sec  
 Attenuation = 64  
 Heating Interval = 60 min  
 Mesh Size = 60/100

TABLE 14  
Sunbury Shale

Sample #	Sample Weight	% H.V.	% L.V.	% Wt. Loss	C/M
1) 214	5.36	26.61	73.38	9.33	175.1
2) 215	4.94	31.39	68.61	16.4	204.0
3) 217	4.88	28.51	71.49	12.5	193.6
4) 218	4.37	25.34	74.66	13.7	158.3
5) 219	4.52	27.33	72.67	11.5	147.5
6) 220	3.77	25.72	74.28	16.7	184.9
7) 221	3.41	26.54	73.46	13.2	167.5
Mean	4.46	27.35	72.65	13.3	175.8
S.D.	...	1.911	1.911	2.42	18.41

Ceiling Temperature = 500°C  
 Heating Rate = 120°C/min  
 Attenuation = 64  
 Heating Interval = 60 min  
 Mesh Size = 60/100

TABLE 15  
Sunbury Shale

Sample #	Sample Weight	% H.V.	% L.V.	% Wt. Loss	C/M
1) 222	4.61	28.91	71.81	9.33	176.6
2) 223	4.70	27.07	72.93	8.94	150.5
3) 224	4.49	28.34	71.66	11.80	177.1
4) 225	5.25	31.85	68.15	10.48	154.2
5) 226	4.47	31.13	68.87	10.51	159.0
6) 227	3.71	28.68	71.39	9.97	169.7
7) 228	5.19	26.11	73.89	9.63	167.3
8) 229	3.81	29.93	70.07	10.24	162.1
9) 230	4.08	31.39	68.61	10.54	163.0
10) 231	3.85	31.27	68.73	9.09	153.8
11) 232	4.51	29.75	70.25	13.30	162.0
12) 233	3.77	28.90	71.10	12.20	177.8
Mean	4.37	29.38	70.62	10.50	164.4
S.D.		1.743	1.746	1.27	9.028

Ceiling Temperature = 500°C  
 Heating Rate = 300°C/min  
 Attenuation = 64  
 Heating Interval = 60 min  
 Mesh Size = 60/100

TABLE 16  
Sunbury Shale

Sample #	Sample Weight	% H.V.	% L.V.	% Wt. Loss	C/M
1) 259	4.64	26.25	73.75	11.64	161.2
2) 260	5.17	31.48	68.52	11.61	130.3
3) 261	5.11	28.75	71.25	12.32	148.8
4) 262	5.97	30.61	69.39	13.57	141.8
5) 266	5.31	32.45	67.55	13.74	140.5
6) 267	4.86	30.57	69.43	11.11	135.8
7) 268	4.26	31.75	68.25	13.85	153.1
8) 269	5.31	31.26	68.74	13.37	141.8
Mean	5.08	30.39	69.61	12.65	144.2
S.D.		1.869	1.869	1.035	9.208

Ceiling Temperature = 500°C  
 Heating Rate = 100°C/sec  
 Attenuation = 64  
 Heating Interval = 60 min  
 Mesh Size = 60/100

TABLE 17  
Sunbury Shale

Sample #	Sample Weight	% H.V.	% L.V.	% Wt. Loss	C/M
1) 271	4.19	27.22	72.78	17.18	181.1
2) 272	3.94	28.85	71.15	15.23	155.0
3) 273	3.78	25.86	74.14	9.52	151.1
4) 276	4.25	32.74	67.26	12.71	147.4
5) 277	4.36	31.19	68.81	13.07	151.0
6) 278	1.45	30.54	69.46	12.83	137.7
7) 280	3.94	29.20	70.80	13.71	158.4
8) 281	4.37	27.10	72.90	10.98	129.5
Mean	3.79	29.09	70.91	13.15	151.4
S.D.		2.174	2.174	2.209	14.26

Ceiling Temperature = 500°C  
 Heating Rate = 600°C/sec  
 Attenuation = 64  
 Heating Interval = 60 min  
 Mesh Size = 60/100

the quartz tubes during post-pyrolysis handling. The weight loss results are also tabulated in Table 8 through 17.

Samples of the spent shale (shale after pyrolysis) were subjected to carbon-hydrogen-nitrogen analysis and thermogravimetric analysis by the Institute for Mining and Minerals Research, Lexington, Kentucky. The results of the analysis on the spent Cleveland shale are summarized in Table 18 and the results of the analysis on the spent Sunbury shale are given in Table 19.

In addition to investigating the effects of ceiling temperature and heating rate, the effect of particle size (mesh size) on the overall product yield and distribution on pyrolysis was studied. Samples of Cleveland shale in -30, 30/60, 60/100 and -100 mesh size were prepared by the Institute for Mining and Minerals Research, Lexington, Kentucky. These samples were pyrolyzed at a heating rate of 500°C per second to a ceiling temperature of 650°C for an interval of 20 seconds. The results of these experiments on the -30, 30/60, 60/100, and -100 mesh shale are given in Tables 20, 21, 22 and 23.

As before, samples of the spent shale in the various mesh sizes were subjected to elemental and thermogravimetric analysis by the Institute for Mining and Minerals Research, Lexington, Kentucky. The results of these analyses are given in Table 24.

TABLE 18

Analysis of the Spent Shale as a Function of the Heating Rate  
Cleveland Shale

Heating Rate	Number of Runs	% Carbon	% Hydrogen	% Nitrogen	
10°C per min.	7	10.29 (1.08)	0.75 (0.23)	0.43 (0.07)	
120°C per min.	8	9.85 (0.29)	0.74 (0.07)	0.44 (0.04)	
300°C per min.	6	9.24 (0.29)	0.71 (0.04)	0.44 (0.03)	
100°C per sec.	4	10.80 (1.11)	0.93 (0.19)	0.38 (0.08)	
>500°C per sec.	5	10.55 (0.39)	0.91 (0.28)	0.25 (0.06)	
		% Moisture	% Volatile Matter	% Fixed Carbon	% Ash
10°C per min.	6	0.55 (0.12)	7.2 (1.5)	7.6 (0.4)	84.6 (1.2)
120°C per min.	6	0.67 (0.02)	6.4 (0.4)	7.7 (0.2)	85.2 (0.5)
300°C per min.	4	0.50 (0.17)	5.6 (0.9)	7.1 (1.0)	86.9 (1.5)
100°C per sec.	4	0.70 (0.15)	5.9 (0.2)	7.8 (0.3)	85.6 (0.3)
>500°C per sec.	-	---	---	---	---

Ceiling Temperature = 500°C

Pyrolysis Interval = 60 minutes

Standard deviation (1 sigma) is given in ( ) beside each value

TABLE 19

Analysis of the Spent Shale as a Function of the Heating Rate  
Sunbury Shale

Heating Rate	Number of Runs	% Carbon	% Hydrogen	% Nitrogen	% Moisture	% Volatile Matter	% Fixed Carbon	% Ash
10°C per min.	10	10.72 (.54)	0.87 (.08)	0.42 (.08)				84.7 (0.8)
120°C per min.	7	9.74 (.49)	0.72 (.07)	0.41 (.05)				85.1 (0.6)
300°C per min.	6	9.61 (.35)	0.72 (.03)	0.48 (.01)				86.7 (1.8)
100°C per sec.	4	11.49 (2.0)	0.88 (.21)	0.34 (.11)				85.5 (0.6)
>500°C per sec.	4	10.24 (.40)	0.76 (.09)	0.38 (.05)				85.5 (0.4)
10°C per min.	7	--	6.6 (0.7)	8.7 (0.3)				84.7 (0.8)
120°C per min.	7	0.27	5.8 (0.5)	8.8 (0.3)				85.1 (0.6)
300°C per min.	4	0.39	5.6 (1.0)	7.5 (1.2)				86.7 (1.8)
100°C per sec.	5	0.45	5.5 (0.3)	8.5 (0.4)				85.5 (0.6)
>500°C per sec.	3	0.29	6.1 (0.3)	8.1 (0.1)				85.5 (0.4)

Ceiling Temperature = 500°C

Pyrolysis Interval = 60 minutes

Standard Deviation (1 sigma) is given in ( ) beside each value

TABLES 20-23: Experimental Results of Effects of Mesh  
Size on Cleveland Shale.

TABLE 20  
Cleveland Shale

Sample #	Sample Weight	% H.V.	% L.V.	% Wt. Loss	C/M
1) 319	4.72	38.16	61.84	10.59	106.7
2) 321	4.34	38.39	61.61	9.47	108.7
3) 323	3.68	39.24	60.76	11.41	118.5
4) 324	4.61	40.56	59.44	10.63	99.6
5) 326	4.48	38.51	61.49	14.73	121.0
6) 327	4.27	36.93	63.07	6.79	95.3
7) 328	4.60	39.30	60.70	8.70	84.8
8) 329	4.29	35.22	64.78	8.16	78.4
Mean	4.37	38.29	61.71	10.1	102.
S.D.	...	1.518	1.518	2.26	14.2

Ceiling Temperature = 650°C  
 Heating Rate = 500°C/sec  
 Attenuation = 64  
 Heating Interval = 20 sec  
 Mesh Size = -30

TABLE 21  
Cleveland Shale

Sample #	Sample Weight	% H.V.	% L.V.	% Wt. Loss	C/M
1) 295	3.49	39.01	60.99	9.46	113.5
2) 297	3.44	40.92	59.08	7.56	105.2
3) 298	3.30	43.27	56.73	13.33	118.9
4) 300	3.03	42.40	57.60	9.57	131.5
5) 302	3.57	47.38	52.62	11.2	113.4
6) 303	3.46	46.74	53.26	11.85	107.1
7) 305	3.03	43.64	56.36	12.54	104.3
Mean	3.33	43.34	56.66	10.8	113.4
S.D.	...	2.764	2.764	1.87	8.845

Ceiling Temperature = 650°C  
 Heating Rate = 500°C/sec  
 Attenuation = 64  
 Heating Interval = 20 sec  
 Mesh Size = 30/60

TABLE 22

## Cleveland Shale

Sample #	Sample Weight	% H.V.	% L.V.	% Wt. Loss	C/M
1) 343	4.59	39.79	60.21	14.16	106.0
2) 344	4.58	36.01	63.99	10.70	105.3
3) 345	4.58	37.65	62.35	11.14	102.3
4) 348	4.62	34.73	65.27	10.82	124.9
5) 349	4.38	36.29	63.71	...	118.4
6) 351	4.79	39.76	60.24	11.48	122.0
7) 352	4.63	35.98	64.02	12.74	115.9
8) 353	4.46	39.28	60.72	12.11	112.6
Mean	4.58	37.43	62.56	10.39	113.4
S.D.	...	1.843	1.843	1.876	7.777

Ceiling Temperature = 650°C  
 Heating Rate = 500°C/sec  
 Attenuation = 64  
 Heating Interval = 20 sec  
 Mesh Size = 60/100

TABLE 23

## Cleveland Shale

Sample #	Sample Weight	% H.V.	% L.V.	% Wt. Loss	C/M
1) 330	4.64	37.66	62.34	9.91	105.7
2) 334	4.53	38.65	61.35	10.38	110.1
3) 335	4.75	43.31	56.69	9.68	105.2
4) 338	4.74	37.62	62.38	8.23	78.7
5) 339	4.54	40.76	59.24	14.76	103.8
6) 340	4.67	41.60	58.40	6.85	83.6
7) 341	4.65	37.81	62.19	6.45	80.2
Mean	4.65	39.63	60.37	9.47	95.3
S.D.	...	2.111	2.111	2.579	12.7

Ceiling Temperature = 650°C  
 Heating Rate = 500°C/sec  
 Attenuation = 64  
 Heating Interval = 20 sec  
 Mesh Size = -100

TABLE 24  
 Analysis of the Spent Shale as a Function of the Mesh Size  
 Cleveland Shale

Heating Rate	Number of Runs	% Carbon	% Hydrogen	% Nitrogen
-30	---	---	---	---
30/60	4	11.15 (0.53)	1.08 (0.17)	0.21 (0.12)
60/100	6	9.67 (0.35)	0.85 (0.05)	0.47 (0.02)
-100	4	10.36 (1.03)	0.96 (0.12)	0.41 (0.04)

	% Moisture	% Volatile Matter	% Fixed Carbon	% Ash
-30	0.05	7.1 (0.8)	7.8 (0.2)	84.6 (1.0)
30/60	0.22	6.5 (0.8)	7.7 (0.5)	85.6 (1.2)
60/100	---	---	---	---
-100	0.20	9.3 (0.4)	7.0 (0.4)	83.6 (0.7)

Ceiling Temperature = 650°C  
 Heating Rate = 500°C per sec  
 Pyrolysis Interval = 20 sec  
 Standard deviation (1 sigma) is given in ( ) beside each value

## DISCUSSION

The calibration work on Kraton 1107 Copolymer (Shell Chemical Co., Houston, Texas) indicates that for the 10 second pyrolysis interval the ceiling temperature experienced by the shale is significantly less than the set-point temperature on the pyroprobe, Table 4. Chemical Data Systems reports a thermal time constant of approximately 3 seconds for the coil probe and quartz tube assembly. One would expect, therefore, that the longer the time interval (pyrolysis interval), the closer the actual ceiling temperature to the set-point temperature of the pyroprobe. The work using 60 minute pyrolysis intervals should have an actual ceiling temperature very close to the set-point value.

Previous experimental work along with the calibration experiments discussed above suggests that pyrolysis intervals of 20 seconds or longer are required for optimum pyrolysis of the oil shale samples. In order to utilize the longer pyrolysis intervals and slower heating rates, a Chemical Data Systems Model 310 Concentrator with a trap-purge assembly was employed. This system allows the pyrolysis products generated over the course of the pyrolysis interval to be collected and then, by means of pulse heating the trap to 250°C, slug injected into the injection port of the gas chromatograph.

The first experiments utilizing the Model 310 Concentrator were to serve two purposes:

1. To duplicate experiments previously done to check the performance of the device.
2. To verify the effect of increasing ceiling temperature on the eastern oil shale.

The results of the pyrolysis of Sunbury Shale (60/100 mesh) at 550°C, 650°C and 750°C, are summarized in Table 25. These experiments were all carried out at a heating rate of 500°C/sec for a pyrolysis interval of 20 seconds. The volatile products were collected in the Model 310 Concentrator Trap, pulse heated to 250°C and back-flushed directly into the injector port of the gas chromatograph.

The results obtained using the Model 310 Concentrator compared very favorably with previous experiments by Sturgeon and confirmed the trends previously reported.<sup>(55)</sup> The overall product yield was observed to increase with increasing ceiling temperature (pyrolysis temperature). This trend was observed from both the integrator counts of product per milligram of shale pyrolyzed and from the percent weight loss recorded for the spent shale.

In addition, the molecular weight distribution in the product appeared to be shifted in favor of the lighter and more volatile products at the higher ceiling temperature.

To explain why the overall yield increased as the temperature increased, one may look at a simple molecular model of the kerogen from which shale oil is derived.

TABLE 25

Pyrolysis of Sunbury Shale  
using  
a  
Chemical Data Systems Model 310  
Concentrator

Product Yield and Distribution as a  
Function of Ceiling Temperature

Ceiling Temp.	Number of Runs	% High Volatile	% Low Volatile	Counts per Milligram	% Wt. Loss
550°C	6	28.2 (2.9)	71.8	64.4 x 10 <sup>3</sup> (14.5)	12.9(2.7)
650°C	7	29.9 (2.8)	70.1	108.0 x 10 <sup>3</sup> (11.9)	14.1(1.5)
750°C	4	35.7 (1.6)	65.3	131.8 x 10 <sup>3</sup> (11.2)	16.3(3.7)

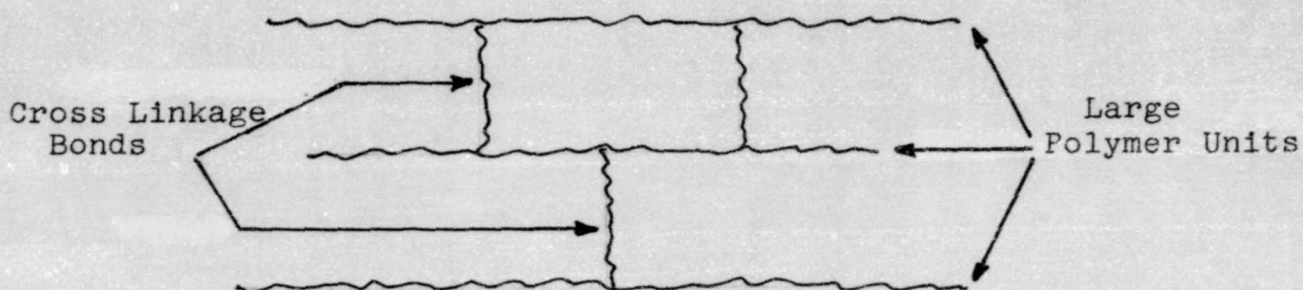
Heating Rate = 500°C per second

Heating Interval = 20 seconds

Attenuation = 64

Standard deviation (1 sigma) is given in ( ) beside each value.

Simple Model of Kerogen



As primary cracking begins at a particular temperature, the crosslinked bonds begin to break. These bonds are the most labile and may consist of benzylic ether, benzylic sulphide and ethylene bridges. (These groups are known to form stable free radicals and will combine with hydrogen).

As the temperature increases, the large polymer units of the kerogen begin to break causing further fragmentation. This fragmentation is called secondary cracking. The additional free radicals that are formed via secondary cracking can react with other combined hydrogen to yield volatile products. An example of this process using model compounds is shown below:

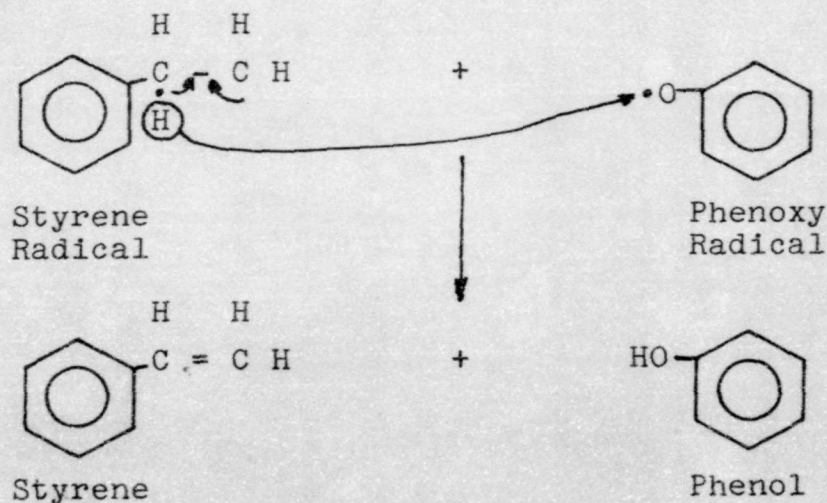
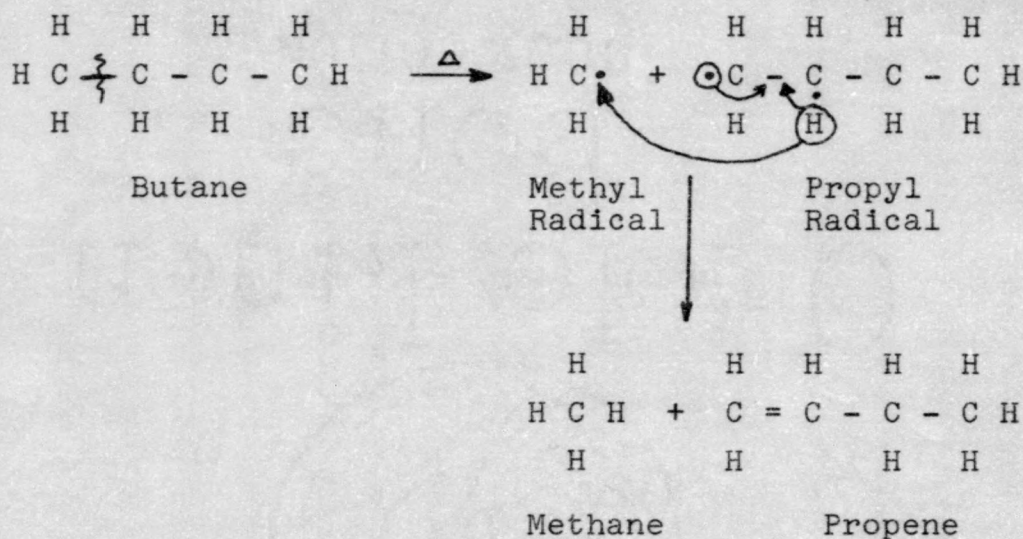


FIGURE 13

These products may then evolve as oil. However, as the temperature increases and as more free radicals are generated, the amount of available hydrogen to "cap" these free radicals declines. When this happens either one of two things can occur.

1. Larger molecules can disproportionate to form gaseous molecules. An example of this could be:



AND

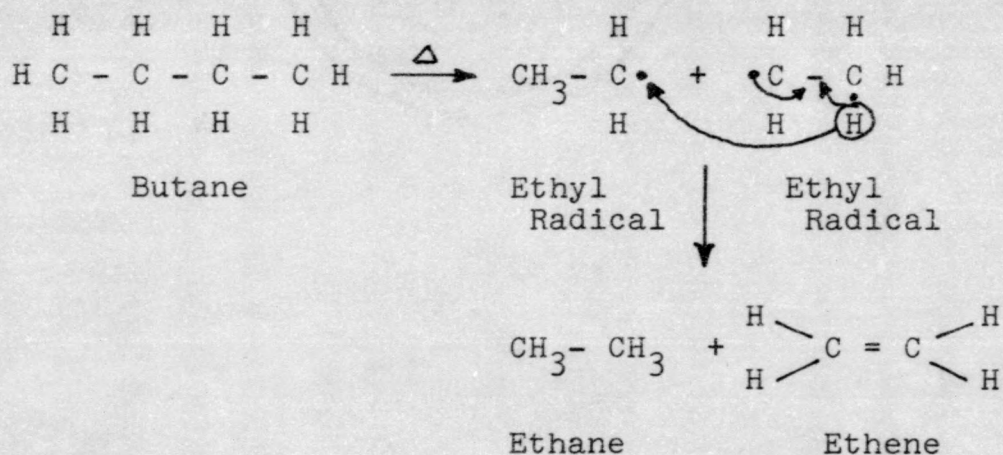


FIGURE 14

As the larger molecules fragment a very large number of products can be formed.

However, the thermally generated free radicals can combine in quite another way as follows:

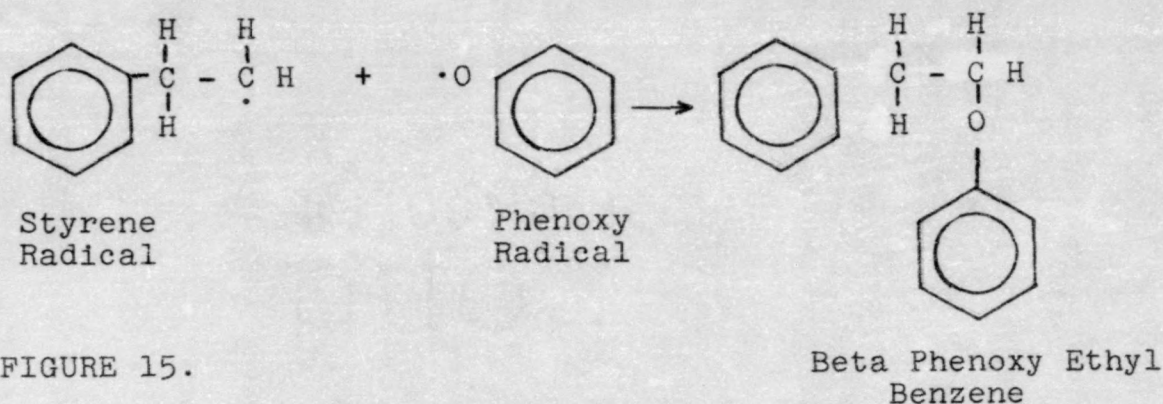


FIGURE 15.

As these radicals could be part of a larger molecule, derived from the kerogen, then the recombination of these kinds of radicals will produce a larger agglomerate called char or coke. As the available hydrogen is depleted the extent of coke formation increases. Many of the eastern oil shales studied appear to be "hydrogen limited" in terms of their ability to form oil or other volatile products.

In addition to work on interval and ceiling temperature, the effect of heating rate (ramp) on the overall product yield and product distribution for the two eastern oil shales was investigated. With the CDS Model 310 Concentrator it is possible to closely approximate Fischer assay conditions on the pyroprobe. It was decided to first collect baseline data under Fischer assay conditions and then to progressively increase the heating rate while holding both the ceiling temperature and pyrolysis interval constant.

The results from the approximate Fischer assay experiments are summarized in Tables 26 and 27. It should be noted that the product distribution between high volatiles and low volatiles is very similar for both shales under these operating parameters. Sunbury, as expected, gave a higher overall yield than Cleveland ( $162.7 \times 10^3$  cts/mg versus  $123.8 \times 10^3$  cts/mg) under the same set of conditions.

After a reasonable set of data had been collected for both shales at  $10^\circ\text{C}/\text{minute}$ , both shales were subjected to pyrolysis at  $120^\circ\text{C}/\text{minute}$ ,  $300^\circ\text{C}/\text{minute}$ ,  $100^\circ\text{C}/\text{second}$  and a nonlinear range of approximately  $600^\circ\text{C}/\text{sec}$ . The ceiling temperature was held constant at  $500^\circ\text{C}$  and the pyrolysis interval at 60 minutes for all of these experiments. The results from these experiments are also summarized in Tables 26 and 27.

Samples of the spent shale for each of the ramps described above were subjected to elemental analysis and thermogravimetric analysis. This data was provided by the Institute for Mining and Minerals Research, Lexington, Kentucky, and is summarized in Tables 28 and 29.

The product yield may be estimated from the integrator counts per milligram of shale pyrolyzed and from the residual carbon and volatile matter left in the spent shale. The weight loss data is too variable to be of much use due to post-pyrolysis handling losses.

The quartz wool plugs must be loose fitting in order to allow free passage of the pyrolysis products out of the tube into the injection port of the gas chromatograph. These

TABLE 26  
Cleveland Shale

Heating Rate Ramp	Runs	Average Weight	% H.V.	% L.V.	Cts	Weight Loss
10°/min	11	4.86	27.0 (2.4)	73.0	122.7 (19.1)	10.1 (1.9)
120°/min	9	4.50	29.3 (1.4)	70.7	122.1 (26.4)	16.6 (4.3)
300°/min	11	4.57	30.2 (1.1)	69.6	130.1 (12.4)	11.9 (1.8)
100°/sec	8	4.50	29.1 (2.1)	70.9	122.7 (25.2)	13.5 (2.3)
600°/sec	9	4.05	27.4 (2.7)	72.6	114.2 (13.6)	12.2 (2.7)

TABLE 27  
Sunbury Shale

10°/min	16	4.43	28.0 (2.0)	72.0	162.6 (28.5)	13.3 (2.5)
120°/min	7	4.46	27.3 (1.9)	72.7	175.8 (18.4)	13.3 (2.4)
300°/min	12	4.37	29.4 (1.7)	70.6	164.4 (9.0)	10.5 (1.3)
100°/sec	8	5.08	30.4 (1.9)	69.6	144.2 (9.2)	12.7 (1.0)
600°/sec	8	3.79	29.1 (2.2)	70.9	151.4 (14.3)	13.2 (2.2)

TABLE 28

Analysis of the Spent Shale as a Function of the Heating Rate  
Cleveland Shale

Heating Rate	Number of Runs	% Carbon	% Hydrogen	% Nitrogen	% Moisture	% Volatile Matter	% Fixed Carbon	% Ash
10°C per min.	7	10.29 (1.08)	0.75 (0.23)	0.43 (0.07)				
120°C per min.	8	9.85 (0.29)	0.74 (0.07)	0.44 (0.04)				
300°C per min.	6	9.24 (0.29)	0.71 (0.04)	0.44 (0.03)				
100°C per sec.	4	10.80 (1.11)	0.93 (0.19)	0.38 (0.08)				
>500°C per sec.	5	10.55 (0.39)	0.91 (0.28)	0.25 (0.06)				
					% Moisture	% Volatile Matter	% Fixed Carbon	% Ash
10°C per min.	6	0.55 (0.12)	7.2 (1.5)	7.6 (0.4)				84.6 (1.2)
120°C per min.	6	0.67 (0.02)	6.4 (0.4)	7.7 (0.2)				85.2 (0.5)
300°C per min.	4	0.50 (0.17)	5.6 (0.9)	7.1 (1.0)				86.9 (1.5)
100°C per sec.	4	0.70 (0.15)	5.9 (0.2)	7.8 (0.3)				85.6 (0.3)
>500°C per sec.	-	---	---	---				---

Ceiling Temperature = 500°C

Pyrolysis Interval = 60 minutes

Standard deviation (1 sigma) is given in ( ) beside each value

TABLE 29

Analysis of the Spent Shale as a Function of the Heating Rate  
Sunbury Shale

Heating Rate	Number of Runs	% Carbon	% Hydrogen	% Nitrogen	% Moisture	% Volatile Matter	% Fixed Carbon	% Ash
10°C per min.	10	10.72 (.54)	0.87 (.08)	0.42 (.08)			8.7 (0.3)	84.7 (0.8)
120°C per min.	7	9.74 (.49)	0.72 (.07)	0.41 (.05)			8.8 (0.3)	85.1 (0.6)
300°C per min.	6	9.61 (.35)	0.72 (.03)	0.48 (.01)			7.5 (1.2)	86.7 (1.8)
100°C per sec.	4	11.49 (2.0)	0.88 (.21)	0.34 (.11)			8.5 (0.4)	85.5 (0.6)
>500°C per sec.	4	10.24 (.40)	0.76 (.09)	0.38 (.05)			8.1 (0.1)	85.5 (0.4)
					% Moisture	% Volatile Matter	% Fixed Carbon	% Ash
10°C per min.	7	--	6.6 (0.7)				8.7 (0.3)	84.7 (0.8)
120°C per min.	7	0.27	5.8 (0.5)				8.8 (0.3)	85.1 (0.6)
300°C per min.	4	0.39	5.6 (1.0)				7.5 (1.2)	86.7 (1.8)
100°C per sec.	5	0.45	5.5 (0.3)				8.5 (0.4)	85.5 (0.6)
>500°C per sec.	3	0.29	6.1 (0.3)				8.1 (0.1)	85.5 (0.4)

Ceiling Temperature = 500°C

Pyrolysis Interval = 60 minutes

Standard Deviation (1 sigma) is given in ( ) beside each value

loose plugs sometimes result in the loss of small particles of spent shale during the post-pyrolysis handling and weighing operations.

Both shales appear to generate the maximum overall yield (based on integrator counts and on residual carbon) between 120°C per minute and 300°C per minute. Heating the shales at ramps beyond 300°C per minute results in a greater retention of carbon and a reduced product yield. A plot of the percent carbon removal from the shale vs log of the heating rate is shown in Figure 16.

The percent ash and the percent residual volatile matter in the spent shale tend to confirm the above observations. As more and more of the organic matter (volatile matter) is driven off, there is less and less residual volatile matter left in the shale and more mineral matter (ash) left behind. The ash content of the spent shale reaches a maximum corresponding to a ramp of 300°C per minute.

One likely explanation for this decrease in overall product yield at heating rates beyond the 300°C per minute ramp is coking or carbonization. It should be noted that the percent fixed carbon (nonvolatile carbon) in the spent shale is observed to increase from the 300°C per minute ramp to the 100°C per second ramp.

Raley and coworkers have suggested that the degradation of oil outside the shale particle is the major determinant of oil yield from the pyrolysis of powdered shale.<sup>(46)</sup> Campbell and coworkers have also reported that coking reactions

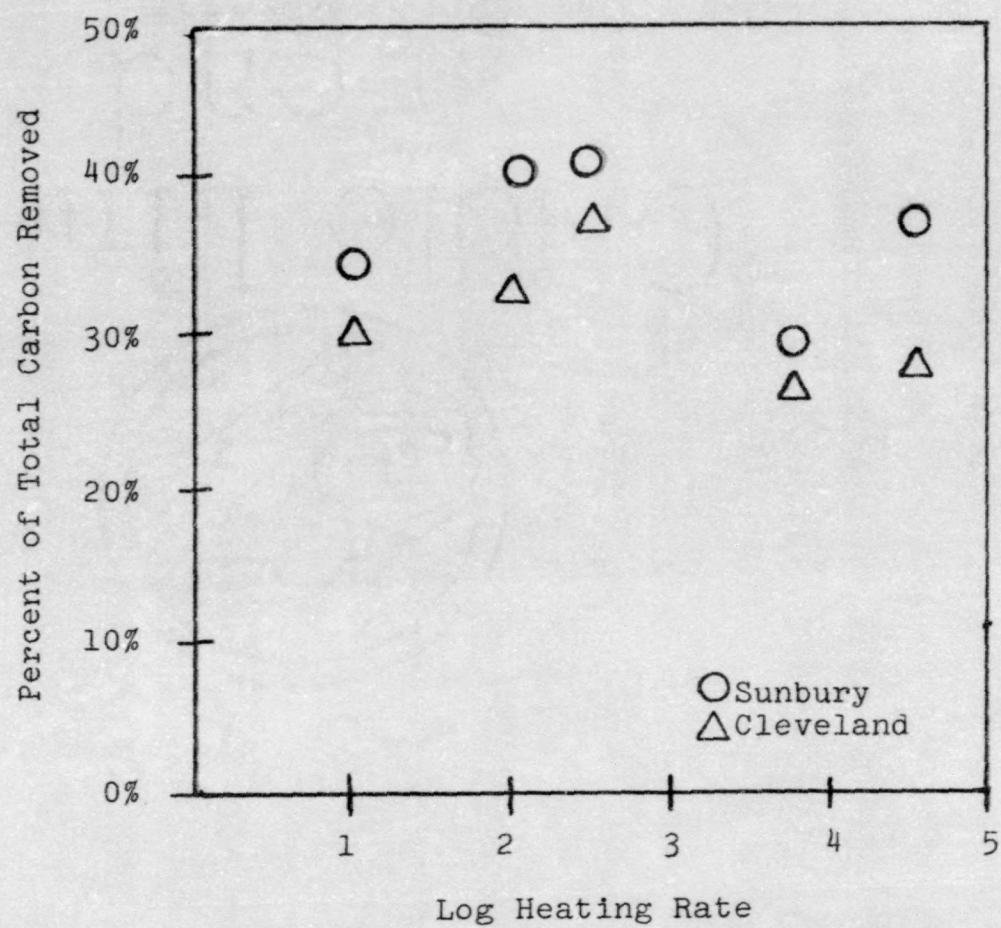


FIGURE 16. Percent Carbon Removal vs. Heating Rate

are the major source of intraparticle oil degradation.<sup>(47)</sup>  
They also report that the rate of coking is strongly dependent upon heating rate.

Finally, there was a great deal of interest in the effect of particle size on the overall product yield and distribution from these two eastern oil shales.

Samples of Cleveland shale in the -30, 30/60, 60/100, and -100 mesh range were obtained from the Institute for Mining and Minerals Research, Lexington, Kentucky. Approximately 4 to 5 milligram portions of these shale samples were subjected to pyrolysis at 650°C for 20 second intervals. A heating rate of 500°C per second was employed in these studies. As before, samples of the spent shale in the various mesh sizes were submitted to the Institute for Mining and Mineral Research, Lexington, Kentucky, for elemental and thermogravimetric analysis. The results from the pyrolysis of the various mesh size samples of Cleveland shale are summarized in Table 30. The elemental analysis and thermogravimetric analysis results on the spent shale samples are summarized in Table 31.

All evidence suggests that the -30 mesh sample gives the lowest overall yield under our experimental conditions. While the differences between the 30/60 and 60/100 samples were small on the pyrogram, weight loss measurements and elemental analysis of the spent shale suggest that the 60/100 mesh samples yield a superior pyrolysis performance.

TABLE 30

Experimental Results  
and Analysis  
of  
Product Yield and Distribution as a  
Function of the Mesh Size

Cleveland Shale

Mesh	Number of Runs	% High Volatile	% low Volatile	Counts per Milligram	% Weight Loss
-30	8	38.3 (1.5)	61.7	101.6 x 10 <sup>3</sup> (14.2)	10.1 (2.3)
30/60	7	43.3 (2.8)	56.7	113.4 x 10 <sup>3</sup> (8.8)	10.8 (1.9)
60/100	8	37.4 (1.8)	62.6	113.4 x 10 <sup>3</sup> (7.8)	11.9 (1.2)
-100	7	39.6 (2.1)	60.4	95.3 x 10 <sup>3</sup> (12.7)	9.5 (2.6)

Ceiling Temperature = 650°C

Heating Rate = 500°C per sec

Pyrolysis Interval = 20 sec

Standard deviation (1 sigma) is given in ( ) beside each value

TABLE 31  
 Analysis of the Spent Shale as a Function of the Mesh Size  
 Cleveland Shale

Heating Rate	Number of Runs	% Carbon	% Hydrogen	% Nitrogen	% Moisture	% Volatile Matter	% Fixed Carbon	% Ash
-30	---	---	---	---				
30/60	4	11.15 (0.53)	1.08 (0.17)	0.21 (0.12)				
60/100	6	9.67 (0.35)	0.85 (0.05)	0.47 (0.02)				
-100	4	10.36 (1.03)	0.96 (0.12)	0.41 (0.04)				
					% Moisture	% Volatile Matter	% Fixed Carbon	% Ash
-30	5	0.05	7.1 (0.8)	7.8 (0.2)				84.6 (1.0)
30/60	5	0.22	6.5 (0.8)	7.7 (0.5)				85.6 (1.2)
60/100	---	---	---	---				---
-100	5	0.20	9.3 (0.4)	7.0 (0.4)				83.6 (0.7)

Ceiling Temperature = 650°C  
 Heating Rate = 500°C per sec  
 Pyrolysis Interval = 20 sec  
 Standard deviation (1 sigma) is given in ( ) beside each value.

The -100 mesh samples did not follow the previous trend. All experimental evidence indicates a decrease in overall yield for the -100 mesh samples. The -100 mesh experiments were repeated with the same result.

There are two possible explanations for the reduced pyrolysis performance of the -100 mesh shale. It is very possible that the organic matter is less efficiently reduced than the mineral matter. Preparation of the -100 mesh samples could yield a product that is richer in mineral matter (poor in organic matter) than the previous samples.

A second explanation is the effect of aging of the -100 mesh shale sample. The finer mesh sample with an increased surface area should, in fact, be more susceptible to the effects of oxidative aging.

Coomes and coworkers have reported that oil shale heated to 70 to 180°C in air gives Fischer assay oil yields which are reduced by as much as 58%.<sup>(48)</sup> They also reported that heating in an oxygen free environment gave unchanged Fischer assay oil yields. The samples of eastern oil shale were not unduly exposed to atmospheric oxygen. However, no special steps were taken to prevent oxidative aging.

To separate the effects of mesh size from the effects of oxidative aging, these experiments must be repeated with fresh shale samples adequately protected.

Finally, several sources of error in these experiments should be noted. The performance of the pyroprobe is dependent upon the parameters of the heating coal. Whenever

the coil becomes deformed, hot spots develop, producing a nonuniform transfer of heat from the coil to the sample. The coil must be inspected prior to each run.

The size of the sample is an important parameter and the sample size should be as uniform as possible. Too small a sample size also results in additional weighing errors.

Likewise, too large a sample size can cause more of a thermal lag in the heat transfer process and can constrict the quartz tube and restrict the evolution of volatile matter.

The quartz tubes holding the shale samples are fitted with loose fitting quartz wool plugs. If these plugs are too large or too tight, the evolution of volatile matter is impeded. If the quartz wool plugs are too loose, there are problems in post-pyrolysis handling and weighing operations, and this results in variations in weight loss percentage.

## SUMMARY

Pyrolysis-gas chromatography experiments indicate that the overall product yield on oil shale pyrolysis increases with increasing ceiling temperature. The product distribution also favors the lighter more volatile materials at the higher ceiling temperature and ramp. In addition, increasing the heating rate for the Sunbury and Cleveland shales above Fischer assay (12° per minute) results in an overall yield enhancement. It would also appear that extremely high heating rates (in excess of 300°C per minute) may also increase the degree of coking or carbonization and result in a decreased overall yield.

Our experiments also suggest that pyrolysis of smaller mesh size shale samples results in an overall yield enhancement. It is also very probable that the finer mesh shale samples are more susceptible to the effects of oxidative aging due to the larger surface area.

In order to separate size and aging effects, more work needs to be done on fresh shale samples of varying mesh size.

## BIBLIOGRAPHY

1. McBrayer J., "Eastern Shale and the Environment," Oak Ridge National Laboratory Review, Fall, 1981, P. 1.
2. Ibid, p. 2.
3. Probststein, R. F. and Hicks, R. E., "Synthetic Fuels," Chemical Engineering Series, McGraw-Hill Book Company, New York, 1976, p. 10.
4. Duncan, D. C., "Oil Shale: A Potential Source of Energy," U.S. Department of the Interior/Geological Survey,
5. Van De Meent, D., Brown, S., Phillip, P., Simoneit, B., "Pyrolysis High Resolution Gas Chromatography and Pyrolysis Gas Chromatography Mass Spectrometry of Kerogens and Kerogen Precursors," Geochim. Soco. Chim. Acta, 44 (7), 999 (1980).
6. McBrayer, J., p. 1.
7. Duncan, D. C., p. 7.
8. Potter, P. E., Maynard, J. B., and Pryor, W. A., "Sedimentology of Shale," Springer-Verlag, New York, Heidelberg, Berlin, pp. 5-7.
9. Franks, F., "Water a Comprehensive Treatise," Vol. 5, Plenum Publishing, Corp. 227 West 17th St., New York, New York, p. 177.
10. Pryor, W. A., "Biogenic Sedimentation and Alteration of Argillaceous Sediments in Shallow Marine Environments," Geol. Soc. Amer. Bull. 86, 1253 (1975).
11. Potter et al., p. 9.
12. Parham, W. E., "Lateral Variations of Clay Mineral Assemblages in Modern and Ancient Sediments," in K. Gekker and A. Weiss, Eds., Proceedings of the International Clay Conference, 1, 136-145 (1966).
13. Edzwald, J. K., and C. R. O'Melia, "Clay Distribution in Recent Estuarine Sediments," Clays and Clay Minerals, 23 39-44 (1975).
14. Middleton, G. V., and M. A. Hampton, "Sediment Gravity Flows: Mechanics of Flow and Deposition," in Turbidites and Deep Water Sedimentation, Soc. Econ. Paleontol. Mineral Pacific Section Short Course, Anaheim, Calif., p. 157, 1973.

15. McKee, E. D. and G. W. Weir, "Terminology for Stratification and Cross-Stratification in Sedimentary Rocks," Geol. Soc. Amer. Bull., 64 381-390 (1953).
16. Potter, P. E. et al., p. 23.
17. Potter, P. E. et al., p. 24.
18. Potter, P. E. et al., p. 25.
19. Potter, P. E. et al., p. 33.
20. Todd, J. E., "Concretions and Their Geologic Effects," Geol. Soc. Amer. Bull., 14, 353-368 (1903).
21. Pettijohn, F. J., Sedimentary Rocks, 3rd Ed. Harper and Row, New York, p. 628.
22. Reiskind, J., "Marine Concretionary Faunas of the Uppermost Bearpaw Shale (Maestrichtian) in Eastern Montana and Southwestern Saskatchewan," in W. G. E. Caldwell, ed., The Cretaceous System in the Western Interior of North America, Geol. Assoc. Canada Spec. paper 13, pp. 235-252.
23. Voight, E., "uber Hiatus - Konkretionen," Geol. Rundschau, 58, 281-296 (1968).
24. Raiswell, R., "The Growth of Cambrian and Liassic Concretions," Sedimentology, 17, 147-171 (1971).
25. Weeks, L. G., "Environment and Mode of Origin and Facies Relationship of Carbonate Concretions in Shales," Jour. Sed. Petrol., 23, 162-173 (1953).
26. Berner, R. A., "Calcium Carbonate Concretions Formed by the Decomposition of Organic Matter," Science, 1959, 195-197 (1968).
27. Potter, P. E., p. 39.
28. Potter, P. E., p. 40.
29. Van De Meent et al., p. 1011
30. Eugster, H. P., and Hardie, L. A., "Sedimentation in an Ancient Playa-Lake Complex: The Wilkin's Peak Member of the Green River Formation of Wyoming," Geol. Soc. American Bull., 86, 319 (1975).
31. Donnell, J. R., "Western United States Oil-Shale Resources and Geology," Symposium papers, Synthetic Fuels from Oil Shale, Atlanta, Georgia, December 3-6, 1979, pp. 17-19.

32. Ibid, p. 27.
33. Probststein, R. F. and Hicks, R. E., p. 10.
34. Duncan, D. C., p. 3.
35. Probststein, R. F. and Hicks, R. E., p. 17.
36. Duncan, D. C., p. 5.
37. Allred, V. D., "Retortive Oil Shales with Super Heated Water Vapor an Emerging Process," Symposium Papers, Synthetic Fuels from Oil Shale, Atlanta, Georgia, Dec. 3-6, 1979, pp. 526-527.
38. Schora, F. C., Janka, J. C., "Progress in Commercialization of the Hytort Process," Eastern Oil Shale Symposium Abstracts, Lexington, Kentucky, October 11-13, 1982, p. 27.
39. Feldkirchner, H. L., Janka, J. C., "The Hytort Process," Symposium papers, Synthetic Fuels from Oil Shale, Atlanta, Georgia, December 3-6, 1979, pp. 499-501.
40. Pforzheimer, H. Jr., "The Current Status of Paraho's Oil Shale Development," Symposium papers, Synthetic Fuels from Oil Shale, Atlanta, Georgia, December 3-6, 1979, p. 475.
41. Kentucky Energy Resource Utilization Program, Institute for Mining and Minerals Research, Kentucky Center for Energy Research Laboratory, Annual Report, July 1, 1979-June 30, 1980, pp. 2-45.
42. Reasoner, J. W., Margolis, M., and Naples, K. V., "Analytical Pyrolysis of Eastern Oil Shales," Symposium papers, Lexington, Kentucky, October 11-13, 1982.
43. D. Gray, J. G. Cogoli, and R. Essen High, Adv. Chemistry Ser. 131, 72 (1974).
44. C. S. Giam, T. E. Goodwin, P. Y. Glam, K. F. Rion and S. G. Smith, Analytical Chemistry, 49, 1540, Sept. 1977.
45. E. J. Levy, "The Analysis of Automotive Paints by Pyrolysis Gas Chromatography," p. 319 (1977).
46. Chemical Data Systems, Technical Paper 081973, Oxford Pennsylvania, 19363.
47. J. K. Whelan, J. M. Hunt, A. Y. Huc., "Applications of Thermal Distillation Pyrolysis to Petroleum Source Rock Studies and Marine Pollution, Chemistry Department, Woods Hole Oceanographic Institution, Woods Hole Mass, 02543, U.S.A., p. 18.
48. Ibid, P. 7.

49. Ibid, p. 23.
50. Ibid, p. 24.
51. Ibid, p. 25.
52. Ibid, p. 26.
53. E. J. Levy, Pittsburgh Conf. on Anal. Chem. and Appl. Spectr., March 1977.
54. J. G. Walker, J. Chromatog. Sci., 6, 267 (1977).
55. Reasoner, J. W., Sturgeon, L. P., Naples, K. V., and Margolis, M., "Analytical Pyrolysis of Eastern Oil Shale," Proceedings of the 1981 Eastern Oil Shale Symposium, Lexington, Kentucky, Nov. 1981, p. 11.
56. Raley, J. H. and Braun, R. L., American Chemical Soc. Meeting, San Francisco, California, Aug. 1976.
57. Campbell, J. H., Koskinas, G. H., Stout, N. D. and Coburn, T. T., In Situ, 2 (1), 1 (1978).
58. Combes, R. M., Sommer, F. H. and Reuben, J. B., Proceeding of the Tenth Oil Shale Symposium, Golden, Co., 1977, p. 200.